Purdue University
Purdue e-Pubs

Birck and NCN Publications | Birck Nanotechnology Center

12-2013

Enhanced reaction rate for gas-phase epoxidation of propylene using H-2 and O-2 by Cs promotion of Au/TS-1

Wen-Sheng Lee
Purdue University, wenshenglee@purdue.edu

M. Cem Akatay
Birck Nanotechnology Center, Purdue University, mcakatay@purdue.edu

Eric A. Stach
Birck Nanotechnology Center, Purdue University, Brookhaven Nationall Lab, eastach@purdue.edu

Fabio H. Ribeiro
Purdue University, fabio@purdue.edu

W.N. Delgass
Purdue University, delgass@purdue.edu

Follow this and additional works at: http://docs.lib.purdue.edu/nanopub

 Part of the Nanoscience and Nanotechnology Commons

Lee, Wen-Sheng; Akatay, M. Cem; Stach, Eric A.; Ribeiro, Fabio H.; and Delgass, W.N., "Enhanced reaction rate for gas-phase epoxidation of propylene using H-2 and O-2 by Cs promotion of Au/TS-1" (2013). *Birck and NCN Publications.* Paper 1546.
http://dx.doi.org/10.1016/j.jcat.2013.05.023

This document has been made available through Purdue e-Pubs, a service of the Purdue University Libraries. Please contact epubs@purdue.edu for additional information.

Journal of Catalysis 308 (2013) 98–113

Contents lists available at SciVerse ScienceDirect

Journal of Catalysis

journal homepage: www.elsevier.com/locate/jcat

Enhanced reaction rate for gas-phase epoxidation of propylene using H_2 and O_2 by Cs promotion of Au/TS-1

Wen-Sheng Lee [a], M. Cem Akatay [b], Eric A. Stach [b,c], Fabio H. Ribeiro [a], W. Nicholas Delgass [a,*]

[a] Forney Hall of Chemical Engineering, Purdue University, West Lafayette, IN 47907, USA
[b] School of Materials Engineering and Birck Nanotechnology Center, Purdue University, West Lafayette, IN 47907, USA
[c] Center for Functional Nanomaterials, Brookhaven National Laboratory, Upton, NY 11973, USA

ARTICLE INFO

Article history:
Received 28 February 2013
Revised 20 May 2013
Accepted 22 May 2013
Available online 22 June 2013

Keywords:
Au/TS-1
Cs promotion
Gold clusters
Propylene epoxidation
Nanoporous materials

ABSTRACT

Gold clusters supported on titanium silicalite-1 (hereafter denoted as Au/TS-1) with high gold loading at ~0.1–0.16 wt%, prepared by the deposition precipitation (DP) method, showed about two times enhancement in the PO rate (~ 300 versus ~ 150 $g_{PO}\ h^{-1}\ kg_{Cat}^{-1}$ at 200 °C), ~10% increase in PO selectivity (~80% versus ~70%) and ~5–10% increase in H_2 selectivity (~20% versus ~10%) when Cs_2CO_3 instead of Na_2CO_3 was used as the precipitation agent. Using Cs_2CO_3 as the precipitation agent caused a fourfold increase in Au uptake efficiency, indicating a strong interaction between Cs and Au in the Au/TS-1 system. XPS/TEM analyses for two Au/TS-1 samples with the same gold loading at ~0.16 wt% but different alkali metals (Cs versus Na) indicate that more Au was retained inside the TS-1 nanopores for the Cs sample. The presence of Cs is, therefore, proposed to help stabilize small gold clusters (<1 nm) inside the TS-1 nanoporous channels at the high gold loading (>0.1 wt%) due to the Cs/Au interaction, resulting in the promotion of PO rate per gram of catalyst. Furthermore, similar apparent activation energy at ~30 kJ $mole^{-1}$ observed for the Au/TS-1 catalysts with the presence of either Cs or Na suggests that the number, but not the nature of the active sites, is changed in the Cs-promoted samples. Finally, regardless of the type of alkali metal (Na or Cs) present in the catalysts, lower Ti content (Si/Ti molar ratio ~100) for Au/TS-1 catalysts was found to favor PO catalytic performance.

© 2013 Elsevier Inc. All rights reserved.

1. Introduction

The discovery that nanoscale gold particles supported on titania (Au/TiO_2) catalyze propylene to propylene oxide (PO) in the presence of hydrogen and oxygen provides a greener and sustainable PO production route as compared to the current major PO production processes (based on chlorohydrin and organic hydroperoxide intermediates) because water, instead of chlorinated organic compound wastes and/or undesired coproducts, is the only significant by-product [1,2]. Increasing the Ti dispersion on the support improved both PO rate and the stability [3–5] and has led to a focus on either mesoporous titanosilicate (Ti-MCM-41, Ti-MCM-48, Ti-TUD) [6–8] or nanoporous titanium silicalite-1 (TS-1) as preferred supports [1,5,9–11]. The PO rate was first improved to ~ 90 $g_{PO}\ h^{-1}\ kg_{Cat}^{-1}$ by using a 3D mesoporous titanosilicate, with barium as a promoter [12]. Later, Au/TS-1 showed a PO rate of ~ 100 $g_{PO}\ h^{-1}\ kg_{Cat}^{-1}$ [10], and the PO rate was further enhanced to ~ 130—140 $g_{PO}\ h^{-1}\ kg_{Cat}^{-1}$ by either introducing defect sites to TS-1 [13], pretreating the TS-1 with NH_4NO_3 before gold deposition [14], or using a solid grinding (SG) method to deposit gold clusters [1,15]. Recently, a PO rate of ~ 160 $g_{PO}\ h^{-1}\ kg_{Cat}^{-1}$, the highest PO rate at 200 °C currently reported in the literature, was achieved by refining the gold deposition precipitation (DP) conditions in the Au/TS-1 preparation [9].

As to the gold active sites for the PO reaction, gold particles with size 2–5 nm were cited for both Au/TiO_2 and other Au/Ti-based oxides by Haruta et al. [16,17]. On the other hand, density functional theory (DFT) calculations and experimental results suggest that nano-gold clusters (<2 nm) can be energetically favorable for the H_2O_2 formation from O_2 and H_2 [18–20]. Since the Au sites in the Au–Ti catalysts for the PO reaction are generally accepted to be responsible for H_2O_2 generation (while the Ti sites catalyze epoxidation) [21,22], small gold clusters inside the TS-1 nanopores can be active sites for the PO reaction if they are in close proximity to Ti. The latter statement was also supported by our DFT calculation results [9–11,23]. Gold clusters with size ~1.4 nm on the external surface of the TS-1 have been proposed to be the dominant gold active sites for the PO reaction in Au/TS-1 [1]. On the other hand, our recent work in which a specially designed silicalite-1 (S-1)-coated TS-1 material was used as the support confirms the activity of the small gold clusters inside the TS-1 nanopores [24]. Therefore, the nature of the gold active sites in Au–Ti catalysts for the PO reaction is still under debate. Herein, we report that the

* Corresponding author. Fax: +1 765 494 0805.
E-mail address: delgass@purdue.edu (W. Nicholas Delgass).

0021-9517/$ - see front matter © 2013 Elsevier Inc. All rights reserved.
http://dx.doi.org/10.1016/j.jcat.2013.05.023

PO rate (per gram of catalyst) of Au/TS-1(121)Cs catalysts (the number in the parenthesis represents Si/Ti molar ratio and Cs indicates that Cs_2CO_3 was used as a precipitation agent during the deposition precipitation (DP) process) can be further enhanced to around two times higher than that of the highest reported PO rate at 200 °C [9]. A specific interaction between the Au and Cs in the Au/TS-1(121)Cs catalysts, which is induced within the nanopores in the TS-1, has also been identified for the first time. It is proposed that the presence of Cs can help stabilize the small gold clusters (<1 nm) inside the TS-1 nanoporous channels at relatively high gold loading (>0.1 wt%), which increases the number of the gold active sites, leading to the significantly higher PO rate per gram of catalyst found. We also show that lower Ti content (Si/Ti molar ratio ~100) in Au/TS-1 catalysts (with either Na_2CO_3 or Cs_2CO_3 as a precipitation agent) favors PO catalytic performance.

2. Experimental methods

2.1. Synthesis of titanium silicalite-1

Titanium silicalite-1 (TS-1) with different Si/Ti molar ratios was synthesized following the same micellar media method reported previously [9,25]. To avoid the variations caused by using different batches of TS-1, multiple batches of TS-1 were synthesized and then mixed to create the TS-1 supply. Therefore, the TS-1 used in this work shares the same physical/chemical properties.

2.2. Synthesis of Au/TS-1

Gold was deposited onto TS-1 by the DP method, and the preparation conditions were similar to those reported in [9]. For a typical Au/TS-1 preparation, 2–4 g TS-1 was added to an aqueous solution (40 mL) of $HAuCl_4{\cdot}3H_2O$ (Alfa Aesar, 99.99%) with concentration ca. 1.75–7.5 g L^{-1}, and the slurry was stirred for 10–30 min at 900 rpm at RT. An appropriate amount of 1 N (1 Normal) aqueous solution of Na_2CO_3 (J.T. Barker Chemical Co.) or 1 M (1 Molar concentration, which is equal to 2 N) aqueous solution of Cs_2CO_3 (Sigma, 99.99%) or K_2CO_3 (Aqua Solutions, ACS) or Rb_2CO_3 (Alfa Aesar, 99%) was then added immediately by pipette to give an alkali/Au molar ratio ~4–5, targeting the final pH of the slurry at the end of the pH adjustment to be ~6–8. The slurry was stirred for 5–6 h at RT to allow the pH to reach the target value, after which the solid was separated by centrifugation and then washed by suspending the catalyst in 50 mL D.I. water and stirring for 1–2 min. Some samples with higher gold loading (>0.1 wt%) were achieved by using longer mixing time (9.5–16 h) at RT. Finally, the catalyst was separated by centrifugation and dried in a vacuum oven at RT overnight. Catalysts were named by gold loading, Si/Ti molar ratio and type of precipitation agent, such that a catalyst with gold loading 0.1 wt%, Si/Ti molar ratio = 121, and prepared by using Cs_2CO_3 as a precipitation agent is 0.1Au/TS-1(121)Cs.

2.3. Synthesis of Ti-Cabosil EH-5

Approximately 15 g of as-received Cabosil EH-5 was added into ~150 mL deionized water (hereafter denoted as D.I. water) to make a thick paste, and the paste was directly dried at 145 °C in a static oven overnight. After drying, ~12 g of dried Cabosil EH-5 was suspended into ~100 mL isopropyl alcohol (IPA, Alfa Aesar, HPLC Grade, 99.7+%) and the slurry was stirred for a few min. An appropriate amount of titanium (IV) butoxide (TBOT, Alfa Aesar, <99%) was then added to give the Ti content ~0.36 wt% of the finished catalyst, which corresponds to ~1.7% of a monolayer of Ti over SiO_2, assuming the Si site density to be 1×10^{15} atoms cm^{-2} and using the measured BET surface area = 265 m^2 g^{-1} (after water treatment). The final solution was stirred at RT for 1 h and then stirred at 85 °C for another 1–2 h (until all the IPA evaporated). The white solid was then calcined at 550 °C for 6 h with a ramping rate 2 °C min^{-1} in a flow of air ~150–200 mL min^{-1} to remove both residual IPA and the organic ligands.

2.4. Synthesis of Cs-TS-1(121), K-TS-1(121) and Cs-TS-1(121)-DP

For Cs-TS-1(121), approximately 8 g of TS-1(121) was mixed with 28 mL D.I. water. After a few minutes of stirring, ~4.4 g $CsNO_3$ (Sigma, 99.99%) was added to the slurry, and the slurry was stirred at 900 rpm at RT overnight. This Cs ion-exchanged TS-1(121) was separated via centrifugation and washed by ~100 mL D.I. water once. The solid was then dried under vacuum at RT overnight. For K-TS-1(121), the preparation procedure was similar to that for Cs-TS-1(121), except ~2.5 g KNO_3 (Aqua Solutions, ACS grade) was added in place of the $CsNO_3$. For Cs-TS-1(121)-DP, the preparation procedure was to mimic the Au deposition process except HCl (Mallinckrodt Baker) instead of $HAuCl_4{\cdot}3H_2O$ (Alfa Aesar, 99.99%) and was used to adjust the pH of the slurry solution. 2 g of TS-1(121) was suspended to an aqueous solution (40 mL) with 9.6×10^{-5} mole of HCl and then an appropriate amount of 1 M aqueous solution of Cs_2CO_3 (Sigma, 99.99%) that gives Cs/Cl molar ratio ~4.2 was then added to the slurry. The slurry was stirred for 5 h at RT, and a few drops of 0.03 M HCl were added to reach the final pH of the slurry ~6.25. The solid was then separated by centrifugation and then washed by suspending the sample in 50 mL D.I. water and stirring for 1–2 min. Finally, the sample was separated by centrifugation and dried in a vacuum oven at RT overnight.

2.5. Post-treatment of fresh Au/TS-1(121)Na by Cs

In order to further understand the effect of Cs promotion, a series of fresh Au/TS-1(121)Na samples with three different gold loadings (0.007, 0.06, and 0.14 wt%) were prepared according to the procedure described above. Once the Au/TS-1(121)Na samples were dried, different concentrations of $CsNO_3$ (Sigma, 99.99%) solution (low, medium and over dosage, approximately ~2 mL) were added to each gold loading of the Au/TS-1(121)Na samples (approximately 1 g) by impregnation and then the Cs dosed samples were dried in a vacuum oven at RT overnight to remove excess water. Those samples were then directly tested under reaction conditions without any pretreatment. The actual Cs/Au molar ratio obtained for the Cs dosed sample was determined by atomic absorption spectroscopy.

2.6. Characterization

The MFI structure of the TS-1 supports was confirmed by the XRD pattern (XRD, Scintag X2 diffractometer, Cu Kα radiation with scanning rate 1.2° min^{-1}). The Ti coordination in TS-1 was evaluated by UV–vis spectroscopy (DRUV–vis, Varian Cary 5000 outfitted with Harrick Praying Mantis optics and using $BaSO_4$ as the reference). Gold particle sizes were determined by high-resolution transmission electron microscopy (HRTEM, FEI Titan, 300 keV) and metal contents retained in the samples (Au, Ti, and alkali metals) were determined using atomic absorption spectroscopy (AAS, Perkin–Elmer AAnalyst 300). BET surface area as well as the pore volume were measured using N_2 adsorption isotherms (Micromeritics ASAP 2000 with samples degassed at 250 °C for at least 8 h before N_2 adsorption). Surface composition was obtained by X-ray photoelectron spectroscopy (XPS) measured with a Kratos Axis Ultra DLD spectrometer using Al Kα monochromatic X-ray radiation at 1486.6 eV and referenced to the Si 2p line at 103.4 eV [26].

2.7. Measurement of PO reaction rates

Catalysts (0.15 g with 60–80 mesh size), mixed with 1–2 g quartz sand (70–80 mesh size), were placed in a Pyrex reactor with inner diameter 10 mm. The reaction temperature was measured by inserting a type-K thermocouple into the catalyst bed. The reactant mixture consisted of 10/10/10/70 vol.% of hydrogen (Praxair, 99.999%), oxygen (Praxair, 99.999%), propylene (Matheson, 99.9%), and nitrogen (Matheson, 99.999%) with a total flow of 35 mL min^{-1}, resulting in a space velocity of 14,000 mL h^{-1} g_{Cat}^{-1}. Epoxidation was carried out at 200 ± 2 °C, reached with a ramping rate of 1–1.5 °C min^{-1}, and the catalysts were directly activated in the reactant mixture without undergoing any pretreatment before the reaction. The reported PO rate and H_2 selectivity in this work were the average values of the first 1–2 h at ~200 °C. The absence of heat transfer and external mass transfer limitations was checked by varying the amount of the dilution (quartz sand) and the catalyst pellet size (Figs. S2 and S3 and detailed information in the SI). Furthermore, the estimated Mears' criteria for both heat and external mass transfer limitation were much smaller than 0.15 (Table S1 and detailed information in the SI). Internal mass transfer limitations can be neglected because the estimated Thiele modulus was smaller than 1 (Table S2 and detailed discussion and information in the SI). All catalysts were tested within 3 days of gold catalyst synthesis to avoid possible on-the-shelf deactivation, which is observed for some gold catalysts [27].

The reactor effluent was analyzed using an Agilent 6890 gas chromatograph (GC) outfitted with an automatic sampling valve and two sample loops. Oxygenated products (PO, ethanal (Et), propanal (Pr), acetone (Ac) and acrolein (An)) were separated using a Supelcowax 10 capillary column (0.53 mm × 60 m) and analyzed via a flame ionization detector, while inorganic products were separated by a Chromosorb 102 packed column (1/8 in. × 8 ft) and analyzed by a thermal conductivity detector. The propylene conversion, H_2 conversion, oxygenate selectivity, CO_2 selectivity, H_2 selectivity, and carbon balances were calculated as follows:

$$\text{Propylene conversion} = \text{moles of}(C_3\text{-oxygenates} + 2/3\ \text{ethanal} + CO_2/3)/\text{moles of propylene in the feed.}$$

$$H_2\ \text{conversion} = \text{moles of } H_2\ \text{converted/moles of } H_2\ \text{in the feed.}$$

$$C_3\text{-oxygenate selectivity} = \text{moles of } C_3\text{-oxygenate/moles of } (C_3\text{-oxygenates} + 2/3\text{ethanal} + CO_2/3).$$

$$\text{Ethanal selectivity} = 2/3(\text{mole of ethanal})/\text{moles of } (C_3 - \text{oxygenates} + 2/3\ \text{ethanal} + CO_2/3).$$

$$CO_2\ \text{selectivity} = 1/3(\text{mole of } CO_2)/\text{moles of } (C_3 - \text{oxygenates} + 2/3\ \text{ethanal} + CO_2/3).$$

$$H_2\ \text{selectivity} = \text{moles of PO/moles of } H_2\ \text{converted}$$

$$\text{Carbon balance} = (\text{moles of C measured from the reactor effluent (which is equal to 3} \times (\text{propylene} + \text{PO} + \text{Pr} + \text{Ac} + \text{An}) + 2 \times \text{ethanal} + CO_2)/\text{moles of C in the feed (which is equal to 3} \times \text{propylene})$$

Carbon balances were better than 96%. Good H_2 signal was obtained by using N_2 as the carrier gas in the GC, but this inhibited the acquisition of an accurate CO_2 calibration curve when the CO_2 concentration was less than ~0.18 vol.% in the gas stream. Therefore, an accurate measurement of CO_2 for some representative samples (Au/TS-1(100)Cs with different gold loadings) was carried out to determine the selectivities of the products. For these measurements, the catalyst was tested in the reactant mixture with N_2 as the GC carrier gas at 200 °C for ~2 h and then the GC carrier gas was switched to He to measure the CO_2 content in the reactor effluent for another hour. After that, the GC carrier gas was switched back to N_2 again and the catalyst was tested for at least another 1 h. We note that all the reaction conditions were maintained during the course of switching the GC carrier gases. Therefore, PO rate, H_2/propylene conversion, moles of the C_3-oxygenates, and ethanal produced were calculated by averaging the value before (2 h at 200 °C) switching the GC carrier gas from N_2 to He and after (1 h at 200 °C) switching the GC carrier gas from He to N_2, while the moles of CO_2 produced (average value over 1 h) were directly measured with He as the GC carrier gas (see Fig. S1 and detailed information in the SI). Once we established an accurate CO_2 calibration curve with the He carrier gas, we were able to produce a CO_2 calibration in N_2 carrier gas that had an error less than 30%. Therefore, the additional CO_2 selectivities reported in this work were the average values of the first 1–2 h at 200 °C and estimated by using the calibration curves just discussed.

3. Results and discussion

3.1. Characterization of titanium silicalite-1

Fig. 1a and b shows XRD patterns and UV–vis spectra of TS-1 with different Si/Ti molar ratios. The orthorhombic unit cell structure of the TS-1 was evidenced by the lack of splitting of the 2θ peak at ~24.6° in the XRD patterns [9,10], and the incorporation of titanium into MFI framework was indicated by the major absorption at around 220–230 nm, characteristic of Ti in tetrahedral coordination [28]. The apparent BET surface area, pore volume, particle size, bulk as well as surface Si/Ti molar ratio of the TS-1 with different Ti contents are summarized in Table 1. No apparent gradient in the spatial Ti distribution was observed for TS-1(100) and TS-1(77) since both surface and bulk Si/Ti molar ratios were found to be similar. All TS-1 samples, regardless of the Ti content, had an average particle size ~280 nm and the corresponding TEM images are available in our previous work [9].

3.2. Effect of alkali on Au/TS-1(121)

Fig. 2a shows PO rate per gram of catalyst for Au/TS-1(121) samples with different gold loadings prepared by using different precipitation agents: Na_2CO_3, K_2CO_3, Rb_2CO_3, and Cs_2CO_3. For the Au/TS-1(121)Na samples, the PO rate per gram of catalyst continued to increase as the gold loading increased up to ~0.08 wt%. However, further increasing the gold loading from 0.08 to 0.18 wt% did not increase the PO rate (per gram of catalyst). Furthermore, very high gold atom efficiency (~ 500 g_{PO} h^{-1} g_{Au}^{-1}, which corresponds to TOR ~ 0.47 $mole_{PO}$ s^{-1} $mole_{Au}^{-1}$) can be achieved at the lowest gold loadings for the Au/TS-1(121)Na samples. Both of these results suggest that the optimum size of gold clusters for the PO reaction is small because gold particle size generally increases with gold loading [9,11].

In addition, DFT calculation results suggest that 3 atom gold clusters inside TS-1 nanopores can be active sites for the PO reaction [23]. Therefore, the Au/TS-1(121)Na samples in the higher gold loading region (>0.1 wt%) might suffer from loss of the optimum gold cluster size for the PO reaction due to sintering of the small gold clusters, thus making further addition of gold less effective and not contributing to increasing the PO rate (per gram of catalyst).

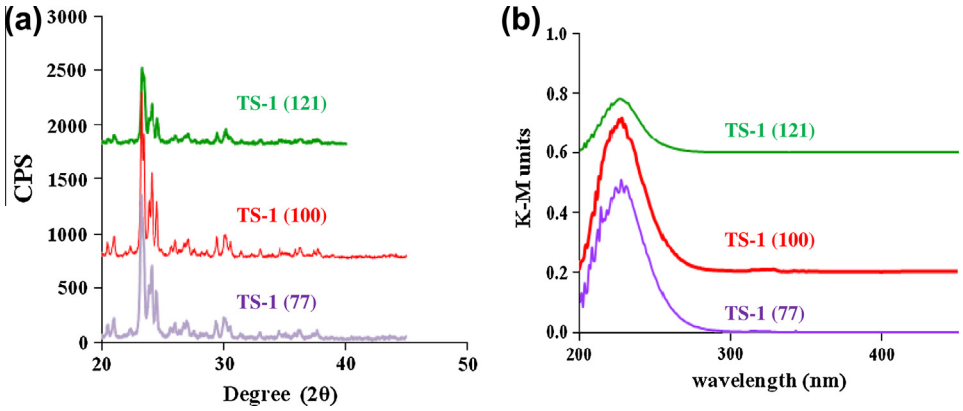

Fig. 1. (a) XRD patterns and (b) UV–vis spectra of TS-1 supports with different Si/Ti molar ratios.

Table 1
Properties of TS-1 with different Si/Ti molar ratios.

Sample[a]	Surface Si/Ti molar ratio[b]	Ti content (wt%)	BET area ($m^2\ g^{-1}$)	Pore volume[c] ($cm^3\ g^{-1}$)	Average particle diameter[d] (nm)
TS-1 (121)	ND	0.65	405 ± 12	0.257	ND
TS-1(100)	102	0.79	398 ± 15	0.243	271 ± 23
TS-1(77)	73	1.02	418 ± 12	0.265	290 ± 34

ND: not determined.
[a] The number in the parenthesis represents the bulk Si/Ti molar ratio determined by AAS.
[b] Determined by XPS analysis.
[c] Pore volume is evaluated from the adsorption isotherm at the relative pressure about 0.97.
[d] Determined by TEM analysis.

Instead of reaching maximum PO rate at $\sim 180\ g_{PO}\ h^{-1}\ kg_{Cat}^{-1}$ at the gold loading ~0.08 wt% as found for Au/TS-1(121)Na samples, the PO rate per gram of catalyst continued to increase to 300—350 $g_{PO}\ h^{-1}\ kg_{Cat}^{-1}$ when the gold loading was increased up to 0.15–0.18 wt% in the presence of Cs, where the corresponding gold atom efficiency is $\sim 200\ g_{PO}\ h^{-1}\ g_{Au}^{-1}$ and the TOR is $\sim 0.19\ mole_{PO}\ s^{-1}\ mole_{Au}^{-1}$. Even though this gold atom efficiency (or TOR based on total moles of Au) is similar to the highest value reported by Haruta and coworkers [1], we note that this level of control of the gold atom efficiency at such a high gold-loading region (>0.15 wt%) for the PO reaction is unprecedented in the literature [1,29]. The TOR of the Au/TS-1(48)Na samples with the gold loading 0.05, 0.1 and 0.25 wt%, prepared by the SG method, was found to be ~0.26, ~0.11 and $\sim 0.04\ mole_{PO}\ s^{-1}\ mole_{Au}^{-1}$ respectively [1], while that for the Au/TS-1 with the gold loading ~0.25 wt%, prepared via immobilizing biosynthesized gold nanoparticles, was even lower at $\sim 0.02\ mole_{PO}\ s^{-1}\ mole_{Au}^{-1}$[29]. Additionally, Fig. 2c shows the reproducibility of 12 Au/TS-1(121)Cs samples (pH value of the gold slurry solution was controlled at ~6–7, gold loading ranged from 0.12 to 0.21 wt% and the Cs/Au molar ratio (retained in the sample) was in the range from 7 to 16), all with PO rate over $200\ g_{PO}\ h^{-1}\ kg_{Cat}^{-1}$ at ~200 °C. Data concerning the selectivities of H_2 and partial oxidation products (PO, ethanal (Et), propanal (Pr), acetone (Ac) and acrolein (An)), propylene and H_2 conversion, and gold atom efficiency ($g_{PO}\ h^{-1}\ g_{Au}^{-1}$) for those twelve samples are available in Table S5 in the SI. It should also be noted that neither K nor Rb matched the promotion by Cs (Fig. 2a). We propose, however, that the nature of the gold active sites in both Au/TS-1(121)Na and Au/TS-1(121)Cs samples is similar, based on the facts that: (1) a similar trend of the gold atom efficiency (PO rate per gram of Au) versus Au loading was observed for both Au/TS-1(121)Na and Au/TS-1(121)Cs samples in the low gold-loading region (<0.08 wt%), as shown in Fig. 2b, and (2) the activation energies for selected Au/TS-1Cs and Au/TS-1Na samples, as shown in Table 2 and Fig. 3, were found to be similar (the corresponding PO rate versus time-on-stream plots for the selected samples for the activation energy measurement are available in Figs. S4–S10 in the SI) and are also in a good agreement with reported values (~25–36 kJ $mole^{-1}$) for the Au/TS-1 catalysts in the literature [10,30,31]. Thus, the extension of the positive proportional relationship between the PO rate per gram of catalyst and the gold loading into the high gold-loading region (>0.1 wt%, Fig. 2a) suggests that the increased PO rate per gram of catalyst for the Au/TS-1(121)Cs samples at the high gold loading was due to an increased number of gold active sites. The gold atom efficiency of the Au/TS-1(121)Cs samples with gold loading 0.1–0.18 wt% was also found to be much higher (by about $\sim 100\ g_{PO}\ h^{-1}\ g_{Au}^{-1}$) than that of the Au/TS-1(121)Na samples in the same Au loading range (Fig. 2b). Therefore, we propose that the presence of Cs can stabilize small gold clusters in the high gold-loading region (>0.1 wt%) in Au/TS-1 catalysts. Moreover, the promotion effect of Cs, observed only in the high gold-loading region (>0.1 wt%, Fig. 2a), was also verified by the following Cs post-addition experiments.

Au/TS-1(121)Na samples with three different gold loadings (0.14, 0.06, and 0.007 wt%) were prepared prior the addition of Cs. Once the Au/TS-1(121)Na samples were dried, different amounts of $CsNO_3$ (Cs/Au molar ratios, determined afterward by AAS, ranged from 0 to 84) were impregnated onto each sample as described in the Experimental methods section. The extent of the promotion by Cs was found to be a function of the gold loading. The most apparent promotion effect was observed for the 0.14Au/TS-1(121)Na sample, whereas Cs had no promotion effect on the 0.007 Au/TS-1(121)Na sample, as shown in Fig. 4a. If we assume that sintering of the gold clusters at this very low gold loading (~0.007 wt%) can be neglected, the fact that no promotion effect was observed for 0.007Au/TS-1(121)Na with different Cs/Au molar ratios (0–20) (Fig. 4b) suggests that the presence of the Cs does not alter the chemistry of the gold active sites (the small gold clusters < 1 nm). Furthermore, we note that, as will be discussed later,

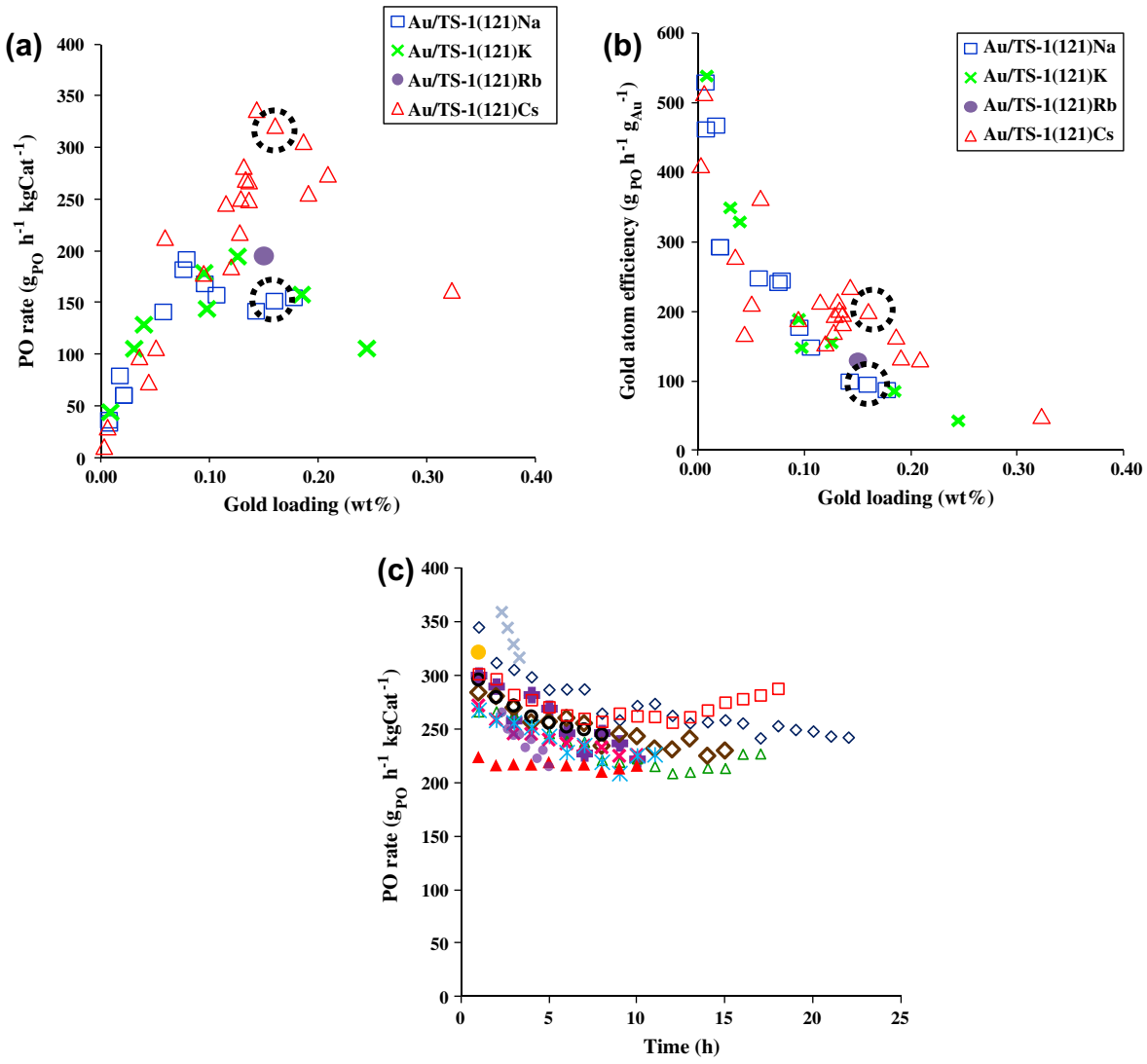

Fig. 2. (a) PO rate per gram of catalyst and (b) PO rate per gram of gold for Au/TS-1(121) with different gold loadings prepared by using different precipitation agents: Na_2CO_3, K_2CO_3, Rb_2CO_3, and Cs_2CO_3. The data were taken as the average values of the first 1–2 h at 200 °C. The circled data points were the rates right at ~200 °C (reacted at ~200 °C for less than 0.5 h). (c) Reproducibility of the PO rates for twelve Au/TS-1(121)Cs catalysts prepared as listed in Table S5 of the SI.

Table 2
Kinetic performance of selected Au/TS-1 samples for propylene epoxidation.

Catalysts	Si/Ti molar ratio (SD < 3%)[a]	Au loading (wt%) (SD < 10%)[a]	Ea (kJ $mole^{-1}$)[b]	PO rate($g_{PO}h^{-1}kg_{Cat}^{-1}$)[c] (SD < 6%)
0.013Au/TS-1(121)Na	121	0.013	32.5 ± 0.8	69
0.016Au/TS-1(121)Na	121	0.016	30.3 ± 1.6	81
0.10Au/TS-1(121)Na	121	0.10	31.4 ± 1.1	174
0.16Au/TS-1(121)K	121	0.16	28.5 ± 1.0	153
0.14Au/TS-1(121)Cs	121	0.14	30.5 ± 2.8	337
0.03Au/TS-1(77)Cs	77	0.03	31.7 ± 1.6	62
0.76Au/TS-1(77)Cs	77	0.76	30.1 ± 0.9	314

[a] SD = standard deviation.
[b] PO rate versus time-on-stream plot of each sample is available in Figs. S4–S10 in the SI.
[c] Rates are the average value of first 1–2 h at 200 °C and 11–12th h at 200 °C for 0.03Au/TS-1(77)Cs. Reaction conditions: $H_2/C_3H_6/O_2/N_2$ = 3.5/3.5/3.5/24.5 mL min^{-1}, space velocity = 14,000 mL h^{-1} g_{Cat}^{-1}.

no apparent gradient of the gold species spacial distribution throughout the whole TS-1 volume was found for the freshly made Au/TS-1 samples (with either Na_2CO_3 or Cs_2CO_3 as a precipitation agent). Therefore, the significant promotion for the 0.14Au/TS-1(121)Na sample with the addition of Cs indicates that the presence of Cs can help the stabilization of the existing small gold clusters inside the TS-1 nanopores for a sample with high gold loading, thus increasing the number of the active sites.

A detrimental effect of Cs started to appear when the Cs/Au molar ratio was higher than ~40 in these Cs post-added Au/TS-1(121)Na samples (Fig. 4b). It should be noted that this limiting Cs/Au molar ratio was obtained when Cs was post-added to the

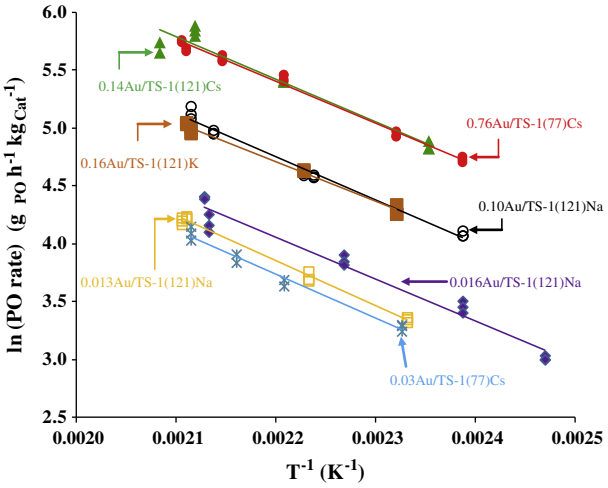

Fig. 3. Arrhenius plot of selected Au/TS-1 catalysts with different gold loadings (which correspond to different PO rates per gram of catalyst), Ti contents, and precipitation agents. PO rate versus time-on-stream plot of each sample is available in Figs. S4–S10 in the SI.

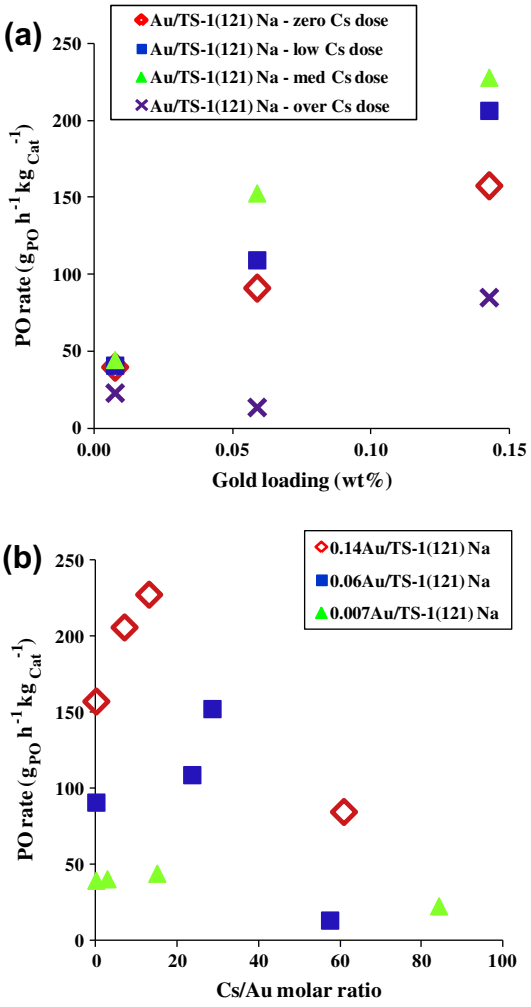

Fig. 4. (a) PO rate as a function of gold loading and (b) PO rate as a function of Cs/Au molar ratio (retained in the samples) for the Au/TS-1(121)Na samples with different gold loadings (0.14, 0.06 and 0.007 wt%) impregnated with different amounts of $CsNO_3$ that correspond to the zero dose, low dose, medium dose, and over dose shown in Fig. 4a.

Au/TS-1(121)Na samples, while the Cs/Au molar ratios and performance of selected Au/TS-1(121)Cs samples (in which Cs could interact with Au in the initial catalyst DP slurry solution) are listed in Table 3. The PO rate enhancement via direct initial mixing with Cs and Au during the DP process (0.14Au/TS-1(121)Cs with Cs/Au molar ratio ~13 and PO rate ~ 268 g_{PO} h^{-1} kg_{Cat}^{-1}, Table 3) was also found to be slightly superior to that via the post-addition of Cs (0.14Au/TS-1(121)Na post-added with Cs, resulting the Cs/Au molar ratio ~13 and PO rate ~ 228 g_{PO} h^{-1} kg_{Cat}^{-1}, Fig. 4b). The exact reason for this unequal promotion effect is not clear yet. It appears that Cs needs to be in proximity to Au during DP in the TS-1 to give the maximum promotion in either the PO rate per gram of catalyst and/or the gold uptake efficiency. While the Au and Cs are directly in contact during DP, there might be some sites in the TS-1 which Cs can exchange first and this Cs site can further help stabilize Au species inside the TS-1, leading to an increased number of the gold active sites. Moreover, we note that the literature has reported a Cs promotion via a physical mixture of CsCl and Au/Ti-MCM-41 [32], but we found no noticeable promotion for a physical mixture of Au/TS-1(121)Na and CsCl or $CsNO_3$ (Table S3 and Fig. S11 in the SI). This implies that the Cs needs to be proximate to the Au to give a significant promotion effect, which is consistent with the argument that the PO rate promotion requires interaction between Au and Cs occurring at the atomic scale. A slightly decreased PO rate (compared to that for 0.1Au/TS-1(121)Na) was observed for the physical mixture of 0.1Au/TS-1(121)Na and CsCl, which is probably due to the presence of Cl that deactivates gold active sites by promoting agglomeration of gold particles [32]. As to the H_2 selectivity, the H_2 consumption was found to be reduced by about 90% and PO selectivity could be improved to 97% at a propylene conversion of 1.7% in Uphade's physical mixture work [32]. However, both PO and H_2 selectivity of Au/TS-1(121)Na were just slightly improved (Table S3) by physically mixing with either CsCl or $CsNO_3$ in our experiments.

Table 3 shows the PO catalytic performance of Au/TS-1 samples with different Ti contents, gold loadings, and different precipitation agents. For Au/TS-1(121)Na samples, it was found that both PO and H_2 selectivity generally decreased, while the selectivities of oxygenates other than PO (Et, Pr, Ac, and An) and CO_2 generally increased, as the gold loading increased.

This observed trend is in a good agreement with the literature [1] and suggests that larger gold particles tend to promote both CO_2 formation and the isomerization of PO over Au/TS-1. We note that the formation of propane for all the samples prepared and tested at reaction temperature ~200 °C in this work was found to be undetectable. This is consistent with the data reported by Haruta and coworkers [1] and their recent finding that the presence of alkali metal (>100 ppm) in the Au/TS-1 catalyst can switch off the propane formation [17]. In the low gold-loading region (<0.1 wt%), the PO selectivity for both Au/TS-1(121)Na and Au/TS-1(121)Cs samples was similar (86–89%). However, in the high gold-loading region (0.1–0.16 wt%), the PO selectivity of the Au/TS-1(121)Na samples (~64–77%) was about 10% less than that of the Au/TS-1(121)Cs samples (~86–88%), which was the consequence of the higher selectivities in the other oxygenates (Et, Pr, Ac, and An) and CO_2 in the Au/TS-1(121)Na samples (Table 3). This PO selectivity performance of the Au/TS-1(121) samples at the different gold loadings is consistent with our conclusion that the population of small active gold clusters is higher in the Au/TS-1(121)Cs samples in the high gold-loading region (>0.1 wt%) as compared to that for the Au/TS-1(121)Na samples. Furthermore, the ability of Cs to stabilize small gold clusters is also reflected in the higher H_2 selectivity over the Au/TS-1(121)Cs samples (~20%) relative to their Na analogues (12–15%) in the high gold-loading region (0.1–0.16 wt%), because larger gold particles (~2 nm) have been proposed to promote H_2 combustion [6]. Regardless of the type of

Table 3
Propylene epoxidation over Au/TS-1 with different Au, Ti loadings and different precipitation agents.

Catalysts	Metal loading (wt%)[a]			Cs/Au molar ratio[b]	Selectivity[c] (%)							Conversion[c] (%)		PO rate(g_{PO} h^{-1} kg_{Cat}^{-1})[c]	TOR (s^{-1})[c]	
	Ti	Au	Cs		Et	PO	Pr	Ac	An	CO_2[d]	H_2	C_3H_6	H_2		mol_{PO} s^{-1} mol_{Au}^{-1}	mol_{PO} s^{-1} mol_{Ti}^{-1} $/10^{-3}$
0.01Au/TS-1(121)Na	0.65	0.01			1.2	88.6	5.1	0.1	1.1	4.0	40.1	1.2	2.8	36	0.50	1.29
0.08Au/TS-1(121)Na	0.65	0.08			0.8	87.1	1.6	0.4	0.7	9.4	24.0	6.5	23.7	182	0.23	6.44
0.11Au/TS-1(121)Na	0.65	0.11			1.8	77.3	3.8	0.6	2.1	14.4	14.3	6.4	33.2	157	0.14	5.57
0.14Au/TS-1(121)Na	0.65	0.14			2.6	74.6	3.8	1.1	3.3	14.5	12.5	6.2	37.7	142	0.09	5.02
0.16Au/TS-1(121)Na[i]	0.65	0.16			3.1	64.3	5.3	1.1	3.6	22.6	10.6	7.0	44.0	151	0.09	5.34
0.01Au/TS-1(121)Cs	0.65	0.01	1.28	315 (7.3)	1.2	89.7	0.7	0.1	0.0	8.3	18.4	1.1	5.4	30	0.47	1.05
0.04Au/TS-1(121)Cs	0.65	0.04	2.37	100 (7.6)	1.0	87.0	0.9	0.4	0.4	10.2	21.4	3.4	13.8	98	0.26	3.46
0.05Au/TS-1(121)Cs	0.65	0.05	2.55	75 (7.4)	1.2	86.2	1.1	0.3	0.4	10.9	25.4	3.6	12.6	107	0.20	3.77
0.11Au/TS-1(121)Cs	0.65	0.11	1.58	20 (6.6)	1.2	86.4	1.0	0.4	0.9	10.1	20.1	9.1	37.9	246	0.20	8.71
0.13Au/TS-1(121)Cs[f]	0.65	0.13	1.42	16 (6.7)	1.1	85.1	0.9	0.5	1.1	11.1	19.9	9.7	40.4	269	0.20	9.53
0.14Au/TS-1(121)Cs	0.65	0.14	1.19	13 (6.7)	1.1	82.8	1.1	0.6	1.4	13.0	19.1	10.3	43.5	268	0.19	9.48
0.16Au/TS-1(121)Cs[i]	0.65	0.16	ND	ND	1.4	88.8	1.0	0.5	0.0	8.3	24.8	11.4	39.9	320	0.19	11.3
0.19Au/TS-1(121)Cs	0.65	0.19	1.37	11 (6.8)	1.2	80.4	1.0	0.7	1.4	15.3	16.2	10.2	49.6	256	0.13	9.05
0.01Au/TS-1(121)K	0.65	0.01			0.8	90.0	1.8	0.3	0.9	6.2	23.1	1.6	6.1	44	0.52	1.56
0.03Au/TS-1(121)K	0.65	0.03			0.9	85.2	0.8	0.3	0.6	12.2	28.1	3.9	11.7	106	0.33	3.73
0.04Au/TS-1(121)K	0.65	0.04			0.9	85.7	1.1	0.3	0.6	11.4	24.4	4.8	17.4	129	0.31	4.56
0.09Au/TS-1(121)K	0.65	0.09			1.0	83.5	1.1	0.5	1.0	12.9	18.4	6.9	31.2	179	0.18	6.33
0.13Au/TS-1(121)K	0.65	0.13			1.2	79.6	1.3	0.7	1.6	15.7	15.2	7.2	38.3	195	0.15	6.89
0.02Au/TS-1(100)Cs [e]	0.79	0.02	0.91	56 (6.3)	1.0	91.0	2.1	0.4	0.8	4.8 [e]	44.9	4.1	7.7	123	0.48	3.57
0.06Au/TS-1(100)Cs [e]	0.79	0.06	0.78	18 (6.1)	1.5	87.5	2.2	0.7	0.9	7.2 [e]	29.7	8.4	24.0	240	0.35	6.98
0.09Au/TS-1(100)Cs [e]	0.79	0.09	1.20	20 (6.1)	1.6	85.0	2.0	0.8	1.0	9.6 [e]	27.9	9.9	29.5	285	0.30	8.31
0.16Au/TS-1(100)Cs [e]	0.79	0.16	1.10	10 (6.3)	1.7	81.0	1.5	1.1	0.6	14.2 [e]	15.9	10.5	53.8	298	0.17	8.66
0.03Au/TS-1(77)Cs	1.03	0.03	0.5	19 (6.0)	2.1	77.2	7.1	1.0	1.4	11.3	20.9	3.0	10.2	71	0.19	1.58
0.11Au/TS-1(77)Cs	1.03	0.11	1.3	17 (6.6)	1.3	85.5	2.8	0.8	0.8	8.9	29.3	6.4	18.1	174	0.15	3.89
0.18Au/TS-1(77)Cs	1.03	0.18	2.4	19 (6.9)	1.2	86.2	1.2	0.7	0.7	10.1	22.8	8.9	32.3	257	0.13	5.74
0.29Au/TS-1(77)Cs[g]	1.03	0.29	2.0	10 (6.6)	2.0	80.0	2.6	1.0	1.3	13.1	28.8	11.7	32.1	311	0.10	6.94
0.76Au/TS-1(77)Cs	1.03	0.76	2.9	6 (6.5)	1.5	79.4	1.3	0.8	1.1	15.9	19.9	12.1	51.0	315	0.04	7.03
0.02Au/TS-1(77)Na[h]	1.03	0.02			1.0	69.9	13.6	0.8	1.9	12.9	19.6	1.2	4.9	26	0.12	0.58
0.03Au/TS-1(77)Na[h]	1.03	0.03			1.2	77.6	10.7	0.7	1.3	8.4	23.9	2.0	6.8	44	0.16	0.99
0.05Au/TS-1(77)Na[h]	1.03	0.05			1.2	74.7	10.9	0.8	1.5	10.9	20.5	2.6	9.3	60	0.10	1.35
0.09Au/TS-1(77)Na[h]	1.03	0.09			1.5	67.9	11.6	1.3	1.9	15.7	13.5	3.3	16.3	72	0.08	1.61
0.13Au/TS-1(77)Na[h]	1.03	0.13			1.4	74.8	6.9	0.5	1.2	15.2	12.5	4.7	27.1	112	0.08	2.49

[a] Bulk metal contents (Cs, Ti and Au) retained in the catalysts were determined by AAS.
[b] The number in the parenthesis represents the final pH value of the gold slurry solution at the end of pH adjustment.
[c] Reaction conditions: $H_2/C_3H_6/O_2/N_2$ = 3.5/3.5/3.5/24.5 mL min^{-1}, space velocity = 14,000 mL h^{-1} g_{Cat}^{-1}. The data were taken as the average values of the first 1–2 h at 200 ± 2 °C.
[d] CO_2 selectivity was estimated by using the known calibration curves and the rate data were taken as the average value of the first 1–2 h at 200 °C (except for the samples with the superscript e).
[e] CO_2 selectivity was obtained by directly measuring the CO_2 content with He as the GC carrier gas. PO rate, H_2, propylene conversion, and the selectivity of all oxygenates are the average value before switching the GC carrier gas from N_2 to He (~2 h at 200 °C) and after switching the GC carrier gas from He to N_2 (~1 h at 200 °C).
[f] The reaction temperature was at 204 °C.
[g] The reaction temperature was at 208 °C.
[h] The reaction temperature ramping rate was ~0.5 °C min^{-1}, and the PO kinetic performance data were taken as the average value between the 3rd to 5th h at 200 °C [9].
[i] The samples were used for XPS analysis (Table 8) and TEM analysis (Figs. 8 and 9). The reported data here were the rates right at reaction temperature ~200 °C (reacted at ~200 °C for less than 0.5 h).

the alkali metal in the Au/TS-1(121) samples, the H_2 selectivity generally decreased as the gold loading increased, which also supports the conclusion that extra H_2 combustion sites are available on the larger gold particles. However, the H_2 selectivities of the Au/TS-1 samples with the lowest gold loadings (~0.01–0.02 wt%) were not always found to give the expected highest H_2 selectivity. The exact reason for this phenomenon remains unclear but might be associated with the balance of the gold species distributed over both Si defect sites and Ti defect sites discussed in [9]. An excess amount of alkali in the catalyst might be another cause of the H_2 selectivity being lower than expected. This is supported by the significantly higher Cs/Au molar ratio (>300) found in the 0.01Au/TS-1(121)Cs sample (Table 3). The literature shows that both CO_2 and H_2 selectivities are functions of the PO rate per gram of catalyst, gold loading, and/or Ti content [1,9]. The generally observed trend is that as the PO rate per gram of catalyst increases (which often corresponds to higher gold loading), the CO_2 selectivity increases but H_2 selectivity decreases. Haruta et al. reported that the H_2 selectivity of 0.05Au/TS-1(48), with a PO rate of 100 $g_{PO}\,h^{-1}\,kg_{Cat}^{-1}$, reached 47%, but as the gold loading further increased to 0.1Au/TS-1(48), with a PO rate 119 $g_{PO}\,h^{-1}\,kg_{Cat}^{-1}$, and 0.25Au/TS-1(48), with a PO rate of 137 $g_{PO}\,h^{-1}\,kg_{Cat}^{-1}$, the H_2 selectivity dropped to 30 and 20%, respectively [1]. Moreover, in the same work [1], the CO_2 selectivity of 0.1Au/TS-1(48), with a gold atom efficiency ~ 119 $g_{PO}\,h^{-1}\,g_{Au}^{-1}$, was ~11%, and the CO_2 selectivities of our 0.13Au/TS-1(77)Na and 0.29Au/TS-1(77)Cs samples with gold atom efficiency ~ 80—100 $g_{PO}\,h^{-1}\,g_{Au}^{-1}$ was ~15% and ~13%, respectively. If we assume that the CO_2 selectivity: (1) is not a strong function of the Ti content (TS-1(48) verses TS-1(77)), (2) is a function of the gold particle size distribution, and (3) that the gold atom efficiency can be roughly predicted from the gold particle size distribution, then the similarity of the CO_2 selectivity of our 0.13Au/TS-1(77)Na and 0.29Au/TS-1(77)Cs samples to that of the 0.1Au/TS-1(48) reported in [1] suggests that the enhanced PO rate in the Au/TS-1Cs catalysts is due to an increase in the number of gold active sites.

Increasing the PO rate per gram of catalyst requires a delicate balance between the Ti content and the gold content (or gold particle size), but optimization of this balance is not necessarily ideal for high H_2 selectivity. Considering that our PO rate per gram of catalyst for the Au/TS-1(121)Cs samples is significantly higher than any reported values, it is surprising that the H_2 selectivity can still be maintained at the level of ~20–25%. Furthermore, the H_2 selectivity of our samples with an Au loading ~0.1 wt% and PO rate ~ 100—150 $g_{PO}\,h^{-1}\,kg_{Cat}^{-1}$ is consistent with the values of 15–30% reported in the literature for samples with similar Au loading and PO rate [1,9]. Further improvement of H_2 selectivity is a long-term goal of research on this catalyst system. Our strategy is trying to first maximize the rate, so that the loss of rate that is likely as H_2 selectivity is optimized will lead to a catalyst with viable values for both rate and selectivity.

3.3. Interaction between Au and Cs in TS-1

A strong interaction between the Au and Cs in the Au/TS-1 samples was first evidenced by the significantly higher gold loading (almost four times) of the Au/TS-1(121)Cs samples versus that for Au/TS-1(121)Na samples even though both samples were prepared under the same preparation conditions, as shown in Table 4. This indicates Cs can help to attract Au into the TS-1. Additionally, the enhancement of the gold uptake efficiency (defined as the gold loading (wt%) in a catalyst divided by the concentration of the gold precursor used for the catalyst preparation) was found to be independent of the pH of the gold solution in the range of pH ~ 7 to ~9. Since electrostatic interaction has been shown to determine the gold loading in Au/TS-1 catalysts [9,33], the effect of electrostatic interaction on the higher gold uptake efficiency in the Cs samples was also examined. Table 5 shows that no significant difference in the gold loading was observed for the gold catalysts we prepared on the supports with very different isoelectric points (IEP), i.e., alumina with IEP ~8 and boron nitride with IEP ~2. The results suggest the higher gold uptake efficiency in the Au/TS-1(121)Cs samples cannot be explained by the electrostatic force between the TS-1 and the Au anion complex. Therefore, one special feature left in the Au/TS-1(121)Cs catalysts is the nanoporous structure (of the TS-1). To identify whether the existence of the nanopores would be a criterion for the significantly higher gold uptake efficiency that occurred in the Au/TS-1(121)Cs samples, a material which contained highly dispersed Ti, analogous to the state of the Ti in the TS-1 but without the nanoporous structure, was prepared. We grafted Ti (Ti loading ~0.36 wt%, corresponding to ~1.7% ML) on Cabosil EH-5, a nonporous material composed of silica nanospheres. The UV–vis spectrum (Fig. 5) showing the major absorption at ~220–230 nm indicates that most of the Ti in that sample was in tetrahedral coordination. The shoulder around 280 nm indicates some of the Ti was in 5-fold or 6-fold coordination, probably due to the coordination to water [34] and/or a small amount of TiOx clusters present in the sample [28]. In order to demonstrate that Ti in 5-fold or 6-fold coordination (in TS-1) is UV–vis sensitive, UV–vis measurement of the TS-1(100) impregnated with 30 wt% H_2O_2 was performed, as it is well known that Ti ions can interact with H_2O_2 to form oxo species [35]. Those higher coordinated Ti species are evident in the broadening of the peaks at 280 nm in spectra in Fig. 5. Even though the Ti in the Ti-grafted EH-5 assumes the tetrahedral coordination of Ti in TS-1, no noticeable difference in the gold loading was found for the samples prepared with this support at similar preparation conditions but with different precipitation agents (Na_2CO_3 versus Cs_2CO_3), as shown in Table 6. The nanoporous structure of TS-1 was, therefore, found to be necessary for inducing the interaction between Au and Cs, which resulted in the higher gold uptake efficiency in the Au/TS-1(121)Cs samples.

To reinforce the argument that there exists a strong interaction between the Au and Cs in Au/TS-1 catalysts, TS-1(121) was first ion-exchanged with either KNO_3 or Cs_2NO_3 (denoted as K-TS-1(121) and Cs-TS-1(121) respectively) and then gold was deposited using the DP conditions described above with Na_2CO_3 as a precipitation agent. Different gold loadings of Au/K-TS-1(121) or Au/Cs-TS-1(121) were achieved by varying the concentration of the gold solution while the Na/Au molar ratio was kept at the value ~4–5 (to target the similar final pH values of the gold slurry, as shown in Table 7). It was found that as the gold loading increased in the Au/K-TS-1(121) samples, the Na loading also increased but the K loading decreased (Table 7). This indicates that either there is no special interaction between Au and K or that Na and K have comparable affinity toward the ion-exchange sites in the TS-1. Therefore, as the Na concentration increased (corresponding to the increased Au loading and the constant Na/Au molar ratio in the preparation solution), more exchanged K was replaced by the Na from the gold solution, resulting in decreased K loading and increased Na loading on the catalyst. Interestingly, the opposite trend was observed in the Au/Cs-TS-1(121) samples for which the Cs loading increased as the gold loading increased, in spite of the increased concentration of Na in the preparation solution. This clearly demonstrates that either Au and Cs has a stronger interaction or that Cs has stronger affinity toward the ion-exchange sites in the TS-1, since otherwise one would expect that the Cs loading would also decrease with the increased Na concentration in the gold solution.

On the other hand, we have found that electrostatic forces, which correspond to the pH of the gold solution, are dominant

Table 4
Preparation conditions used for synthesizing Au/TS-1(121). Different alkali carbonates were used as the precipitation agents and the pH of the gold solution was kept between pH ~ 9 and ~7.5 at RT.

Catalysts	Si/Ti molar ratio	$HAuCl_4$[a] (g)	Precipitation agent	Mixing time (h)	pH	Au loading (wt%)
0.02Au/TS-1(121)	121	0.2096	Na_2CO_3	5	9.00	0.02
0.04Au/TS-1(121)	121	0.2040	K_2CO_3	5	8.80	0.04
0.05Au/TS-1(121)	121	0.2021	Rb_2CO_3	5	8.86	0.05
0.07Au/TS-1(121)	121	0.2153	Cs_2CO_3	5	8.83	0.07
0.06Au/TS-1(121)	121	0.2064	Na_2CO_3	6	7.42	0.06
0.13Au/TS-1(121)	121	0.2108	K_2CO_3	5	7.11	0.13
0.15Au/TS-1(121)	121	0.2073	Rb_2CO_3	5	7.49	0.15
0.22Au/TS-1(121)	121	0.2067	Cs_2CO_3	5	7.50	0.22

[a] The volume of gold solution was ~40 mL for all samples.

Table 5
Preparation conditions used for synthesizing the nano-gold particles supported on either Al_2O_3 or BN for which the isoelectric point (IEP) was reported to be around 8–9 and 2–3 respectively.

Catalysts	Support	$HAuCl_4$[a] (g)	Precipitation agent	Mixing Time (h)	pH	Au loading (wt%)
1.84Au/Al_2O_3	Al_2O_3	0.1148	Na_2CO_3	3.5	6.82	1.84
1.45Au/Al_2O_3	Al_2O_3	0.1101	K_2CO_3	3.5	6.90	1.45
1.88Au/Al_2O_3	Al_2O_3	0.1080	Rb_2CO_3	3.5	6.93	1.88
1.74Au/Al_2O_3	Al_2O_3	0.1093	Cs_2CO_3	3.5	6.80	1.74
0.36Au/BN	BN	0.1065	Na_2CO_3	5	7.11	0.36
0.26Au/BN	BN	0.1178	K_2CO_3	5	7.49	0.26
0.25Au/BN	BN	0.1086	Rb_2CO_3	5	7.64	0.25
0.25Au/BN	BN	0.1061	Cs_2CO_3	5	7.45	0.25

[a] The volume of gold solution was ~40 mL for all samples.

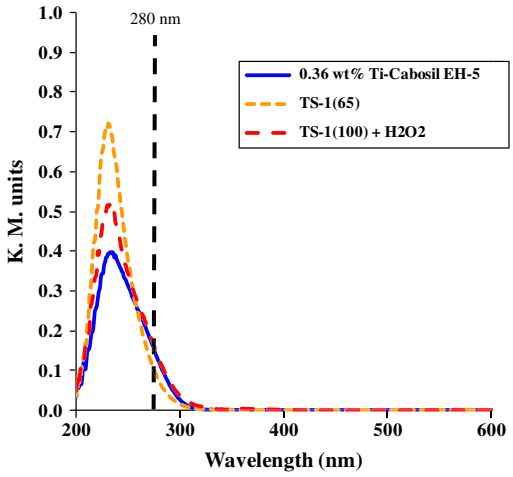

Fig. 5. UV–vis spectra of Ti-Cabosil EH-5 with Ti loading ~0.36 wt%, TS-1(65) and TS-1(100) pretreated by H_2O_2.

for gold deposition, and that the gold loading for two samples prepared at pH ~ 7.5 and 8 with other conditions kept the same was found to be ~0.06% and 0.04%, respectively [9]. This indicates that the Au/Cs-TS-1(121) samples (prepared at pH~8) should have approximately 33% lower gold uptake efficiency as compared to the Au/K-TS-1(121) samples prepared (at pH ~ 7.5). The identical gold loading for the Au/Cs-TS-1(121) and Au/K-TS-1(121) samples, shown in Table 7, supports the conclusion that Cs has a stronger affinity toward Au and can retain Au inside the TS-1, because the pH used for preparing the Cs sample is higher (at ~8). However, the increase in the gold uptake efficiency due to the Cs/Au interaction was much lower in this case, as compared to the samples prepared via regular DP process with Cs_2CO_3 shown in Table 4. This difference is not yet understood, but one explanation is that using Na_2CO_3 as the precipitation agent introduces Na that may destroy and/or dilute the concentration of the Cs sites in the Cs-TS-1(121) by ion exchange and lead to lower gold uptake efficiency.

3.4. Interaction between Cs and Ti in TS-1

Fig. 6 shows the XPS spectra of Ti 2p photoelectrons for the fresh 0.16Au/TS-1(121)Cs and 0.16Au/TS-1(121)Na samples, while the Ti $2p_{3/2}$ peak for the Na sample was found to be symmetric at the binding energy of ~460.0 eV (which is typically assigned to the tetrahedral Ti in the TS-1 [36]), that for the Cs sample showed a shoulder (with a fractional amount of 28%) at lower binding energy ~457.6 eV. No change in the Ti state was found in the XPS spectrum for the spent Na sample (not shown), while the fractional amount of the Ti species assigned to the lower binding energy ~457.6 eV slightly reduced to ~22% for the spent Cs sample (not shown). In order to understand whether or not the presence of Au is indispensible for the observed two different Ti states in the Cs sample, we prepared the following two samples for the XPS measurement: (1) Cs-TS-1(121)-DP, which was prepared by mimicking the Au deposition process except the Au precursor, was not added (see detailed information in the Experimental methods section) and (2) Cs-TS-1(121) pretreated via ion-exchanged by $CsNO_3$ as described above in the Experimental methods section. Interestingly, both samples, Cs-TS-1(121)-DP and Cs-TS-1(121), showed a

Table 6
Preparation conditions used for synthesizing Au/Ti-Cabosil EH-5 using either Na_2CO_3 or Cs_2CO_3 as a precipitation agent.

Catalysts	$HAuCl_4$[a] (g)	Precipitation agent	Mixing time (h)	Prep. temp (°C)	pH	Ti loading (wt%)	Au loading (wt%)
0.21Au/Ti-Cabosil EH-5(Na)	0.1442	Na_2CO_3	7	RT	6.69	0.36	0.21
0.23Au/Ti-Cabosil EH-5(Cs)	0.1414	Cs_2CO_3	7	RT	7.06	0.36	0.23

[a] The volume of gold solution was ~40 mL for both samples.

Table 7
Preparation conditions used and the corresponding properties of the Au/K-TS-1(121) and the Au/Cs-TS-1(121) catalysts. The samples were mixed for 5 h and prepared at RT.

Catalysts	$HAuCl_4$[a] (g)	Precipitation agent	pH	Au loading (wt%)	Na loading (wt%)	K/Cs loading (wt%)
K-TS-1(121)						0.23
0.038Au/K-TS-1(121)	0.1054	Na_2CO_3	7.44	0.038	0.16	0.042
0.063Au/K-TS-1(121)	0.2132	Na_2CO_3	7.45	0.063	0.23	0.028
0.134Au/K-TS-1(121)	0.3292	Na_2CO_3	7.49	0.134	0.28	0.022
Cs-TS-1(121)						1.05
0.046Au/Cs-TS-1(121)	0.1032	Na_2CO_3	8	0.046	0.14	0.35
0.074Au/Cs-TS-1(121)	0.2202	Na_2CO_3	7.78	0.074	0.26	0.52
0.14Au/Cs-TS-1(121)	0.3125	Na_2CO_3	8.22	0.14	0.43	0.57

[a] The volume of gold solution was ~40 mL for all samples.

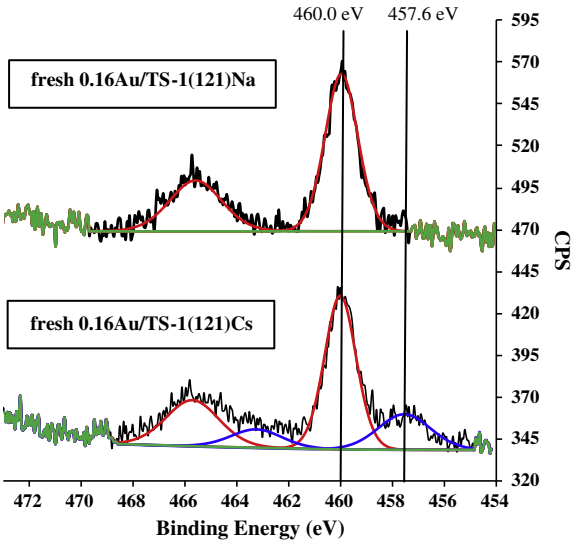

Fig. 6. Ti 2p photoelectron spectra of the fresh 0.16Au/TS-1(121)Na and 0.16Au/TS-1(121)Na samples.

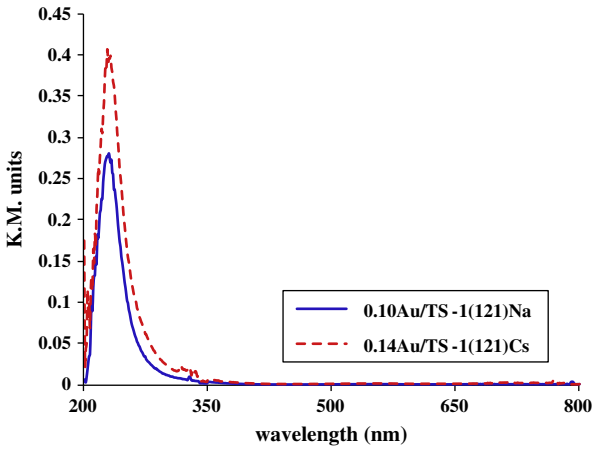

Fig. 7. UV–vis spectra of 0.14Au/TS-1(121)Cs and 0.1Au/TS-1(121)Na.

shoulder at the lower binding energy of ~457.7 eV for the Ti $2p_{3/2}$ peak with fractional amounts of ~18% and ~13%, respectively, suggesting that Cs alone is enough to induce the change in the Ti state in the TS-1. This, of course, does not rule out additional contributions from other factors such as the pH of the pretreatment solution and/or the presence of Au that determine the extent of the change in the Ti state in the TS-1.

The shoulder of the Ti $2p_{3/2}$ peak with lower binding energy ~457.7 eV, observed in the Cs samples, could be attributed to either (1) the reduction of the Ti^{4+} to Ti^{3+} in the framework with tetrahedral coordination, because the standard binding energy for Ti^{3+} is located at 457.7 eV [37] and it has been reported that the Ti in the TS-1 can be reduced [38] or (2) the presence of extraframework Ti for which the corresponding binding energy has been shown to be ~457.8 ± 0.2 eV [36]. Recently, Maurelli and coworkers showed that the Ti^{3+} tetrahedral sites in the framework of TiAlPO-5 gives a broad UV–vis absorption band from ~650 to 1200 nm with the center at ~870 nm [39]. Thus, we turned to UV–vis to examine the existence of the Ti^{3+} in the Cs-promoted Au/TS-1 catalysts. Fig. 7 shows the UV–vis spectra of fresh 0.14Au/TS-1(121)Cs and 0.1Au/TS-1(121)Na samples. No indication of the Ti^{3+} was found in the Cs sample, as suggested by the complete absence of the absorption from 500 to 800 nm, even though the UV–vis spectrum after 800 nm was not available. On the other hand, the amount of extraframework Ti in the 0.14Au/TS-1(121)Cs sample was small, because no significant absorption was observed at either ~280 nm, which is assigned to small TiOx clusters, or ~330 nm, which is assigned to anatase [36]. Considering that the Cs is enriched on the surface (the surface Cs/Ti molar ratio determined by XPS was found to be ~2 times higher than the bulk Cs/Ti molar ratio determined by AAS, Table 8, and XPS is a surface sensitive technique), the observed Ti species with lower binding energy in the Cs sample might occur only in the surface layer where the amount of the Cs is enough to induce the change in the Ti state. In that case, the ~20–40% of the Ti (reduced from Ti^{4+} to Ti^{3+}) in that thin surface layer is not likely to be enough to contribute a significant signal in the UV–vis spectrum.

Since the influence of the Ti chemical state by the presence of Cs was found to be independent of Au, a similar Cs/Ti interaction is expected in the Au/TS-1 catalysts prepared by Haruta and coworkers in which the TS-1 was first pretreated by CsOH before Au deposition by a solid grinding (SG) method [1,15]. Considering that the size of the Au precursor (dimethyl Au(III) acetylacetonate) is too large to enter the TS-1 nanopores, Au was exclusively deposited on the external surface of the TS-1 [15]. Interestingly, no promotion effect was observed in their 0.1Au/TS-1(48)Cs sample, as compared to their other samples pretreated by different alkali bases while at similar gold loading at ~0.1 wt%. This can be explained by the high likelihood that no Au species is available inside their TS-1 nanoporous channels to be stabilized/interacted by the present Cs and is in line with our proposed model for the Cs promotion. Additionally, their experimental observation also suggests that the Cs promotion effect observed in this work cannot be solely attributed to the Cs/Ti interaction.

It is unlikely that the Cs promotion on the PO rate can be attributed to the presence of extraframework Ti in the TS-1, since that Ti species has been shown to be detrimental for both liquid-phase propylene epoxidation [40–42] and the gas-phase PO reaction [4,9]. Furthermore, if the enhanced rate were caused mainly by the promotion of the epoxidation step due to the Cs/Ti interaction

Table 8
Surface (determined by XPS) and bulk composition (determined by AAS) for the two selected samples for 0.16Au/TS-1(121)-Na and -Cs.

Catalysts	Bulk[c] Au/Si molar ratio/10^{-4}	Fresh[d] sample Au/Si molar ratio/10^{-4}	Spent[d] sample Au/Si molar ratio/10^{-4}	Bulk[d] Ti/Si molar ratio/10^{-4}	Fresh[d] sample Ti/Si molar ratio/10^{-4}	Spent[d] sample Ti/Si molar ratio/10^{-4}	Bulk[c] alkali/Si molar ratio/10^{-4}	Fresh[d] sample alkali/Si molarratio/10^{-4}	Spent[d] sample alkali/Si molar ratio/10^{-4}
0.16Au/TS-1(121)Na[a]	4.9	5.8	0.96	83	56	60	22	42	19
0.16Au/TS-1(121)Cs[b]	4.9	2.9	1.8	83	78	63	55	110	120

[a] Preparation conditions: the concentration of gold solution: ~6.3 g$HAuCl_4$ L^{-1}, pH (of the gold slurry): ~6.07, RT, mixing time: ~15 h.
[b] Preparation conditions: the concentration of gold solution: ~1.9 g$HAuCl_4$ L^{-1}, pH (of the gold slurry): ~6.2, RT, mixing time: ~6 h.
[c] Bulk element molar ratio was determined by AAS analysis.
[d] Surface element molar ratio was determined by XPS analysis.

(or even added activity of a specific Cs phase such as the peroxide), the Cs promotion effect (higher rate per gram of catalyst or rate per gram of Au) should also have been observed in the Au/TS-1(121)Cs samples with lower gold loadings at ~0.01 wt% (Table 3) and in the fresh 0.007Au/TS-1(121)Na sample that was post-added with different amounts of Cs (Fig. 4). The fact that such was not the case speaks against assignment of the Cs rate enhancement to Cs/Ti interactions or Cs alone. Having ruled out these direct Cs and Ti contributions, we assign the Cs promotion to an increase in the Au sites for H_2O_2 production or increase in the Au–Ti synergetic sites for the PO production.

3.5. Nature and location of the gold active sites in Au/TS-1(121)

Fig. 8 shows TEM analysis of the fresh 0.16Au/TS-1(121)Cs and 0.16Au/TS-1(121)Na samples. Very few visible gold particles with size ~2–4 nm (too few to allow measurement of the size distribution) were found, indicating that the gold species were highly dispersed (smaller than 1 nm, the detection limit of the HRTEM for these samples) in those fresh samples initially. This finding shows that the higher gold uptake efficiency observed in the Au/TS-1(121)Cs samples (Table 4) is not the result of formation of larger gold particles, but the consequence of attracting gold species more easily into the TS-1 pores. Interestingly, the surface Au/Si molar ratio of the fresh 0.16Au/TS-1(121)Na (Au/Si = 5.8×10^{-4}), determined by the XPS analysis shown in Table 8, is about two times higher than that of the fresh 0.16Au/TS-1(121)Cs (Au/Si = 2.9×10^{-4}). Considering that the gold loading of those two *fresh* samples is the same (with error <10%, Table S4 in the SI), and that there was no noticeable difference in the number as well as the size of the gold particles observed by HRTEM, this significant difference in the surface Au/Si molar ratio indicates that the presence of Cs caused more gold species to be attracted to and to remain in the TS-1 volume, but deeper in the ~280 nm TS-1 particles (estimated from the TS-1 with similar Si/Ti molar ratios in [9]) than could be detected by XPS.

We also note that the bulk Au/Si molar ratios (4.9×10^{-4}), determined by AAS, of above-mentioned two fresh Na and Cs samples were found to be surprisingly close to their corresponding surface Au/Si molar ratios determined by XPS (surface Au/Si molar ratio = 5.8×10^{-4} for the Na sample and 2.9×10^{-4} for the Cs sample), suggesting that the distribution of the gold species was nearly homogeneous throughout the whole TS-1 volume (i.e., including the whole nanoporous channel system in the bulk of the TS-1 crystallites). This statement was further supported by comparing the computed XPS signal intensity ratios (Au/Si) expected for two limiting cases with the same gold loading ~0.16 wt%: (a) gold atoms exclusively deposited on the external surface of the TS-1 and (b) gold atoms homogenously distributed in the entire TS-1 volume. For the case (a): if we assume that the surface of the TS-1 can be regarded as flat (since the coverage of the gold species at ~0.16 wt% on the external surface of the TS-1 would be much smaller than 1 and the diameter of the TS-1 particle is relatively large (~280 nm) as compared to that of a gold atom), the corresponding calculated XPS signal intensity ratio of Au/Si in this scenario was found to be at least 15 times higher than that for the homogeneous distribution in case (b), which would give surface Au/Si molar ratio = the bulk Au/Si molar ratio (see the SI for detailed information). Therefore, the small difference (<2 times) between the surface Au/Si molar ratio and the bulk Au/Si molar ratio observed in the *fresh* 0.16Au/TS-1(121) samples suggests that the gold species *can* diffuse into the TS-1 nanopores and are *not* deposited *only* at the external surface of the TS-1. Furthermore, the local structure of the square-planar Au complex in aqueous solution with different pH (i.e., $[Au(OH)_xCl_{4-x}]^{-1}$, x = 1–4) has been recently studied via

X-ray absorption spectroscopy by Chen et al. [43]. The bond distances were found to be 2.28 Å and 1.98 Å for Au–Cl and Au–O, respectively. Since the two water molecules in the hydration shell were identified to be in the axial position, only the dimensions of the square plane of the Au complex need to be considered to determine whether the Au complex can fit in the TS-1 nanopores. Because the pH of the gold slurry solution for all the Au/TS-1 samples shown in this work was about 6–8, at which 2–3 Cl ligands would be replaced by the OH^- ligands [44], the longest distance across the square-planar structure of the Au complex would be 2.28 + 1.98 = 4.26 Å, slightly smaller than the 5.5 Å diameter of the TS-1 nanopores. Therefore, based on the Au complex structure identified by XAS and the significant chemical potential gradient of the Au complex across the TS-1 in the gold solution, it is possible for the hydrolyzed Au complex to enter the TS-1 nanopores. However, based on the experimental data shown in this work, we cannot rule out the possibility that the major migration of the gold species occurs during the vacuum drying step. We note that the presence of small gold species in the nanopores of Au/TS-1 as-prepared by the DP method was also confirmed by Xe NMR in the recent work published by Haruta and coworkers [15]. The PO catalytic performance of those two samples, evaluated at 200 °C for less than 0.5 h prior to both TEM and XPS analysis, showed that the PO rate of 0.16Au/TS-1(121)Cs was about two times higher than that of 0.16 Au/TS-1(121)Na ($\sim$ 320 versus $\sim$ 150 g_{PO} h^{-1} kg_{Cat}^{-1}).

Fig. 9 shows the TEM images and the corresponding gold particle size distribution of those two samples *after* reaction at 200 °C for less than 0.5 h (the samples were exposed to air prior to the TEM analysis). The average gold particle size was $\sim$3.8 ± 1.6 nm for the spent 0.16Au/TS-1(121)Cs, which is slightly larger than that for the spent 0.16Au/TS-1(121)Na ($\sim$3.3 ± 1.1 nm). Considering that both samples have similar gold loadings and the Cs sample has slightly larger average particle size, one would expect, qualitatively, a lower surface Au/Si molar ratio for the spent 0.16Au/TS-1(121)Cs, compared to that for the spent 0.16Au/TS-1(121)Na, if all the gold species were on the external surface of the TS-1. However, the surface Au/Si molar ratio for the spent 0.16Au/TS-1(121)Cs (Au/Si = 16×10^{-5}) was found to be almost two times higher than that for the spent 0.16Au/TS-1(121)Na (Au/Si = 9.6×10^{-5}) (the samples were exposed to air prior the XPS analysis). This result, combined with the XPS analysis for the *fresh* 0.16Au/TS-1(121)Cs, implies that some of the gold species, originally located deep inside the TS-1, migrated toward the sublayers of the TS-1 during reaction but were still inside the nanoporous channels of the TS-1. Therefore, they did not sinter into large gold particles on the external surface of the TS-1 so were able to contribute to the higher surface Au/Si molar ratio detected by XPS. Furthermore, it should be noted that the density of visible gold particles (# nm^{-2}) was two times higher for the *spent* 0.16Au/TS-1(121)Na (2.1×10^{-3}), compared to that of the *spent* 0.16Au/TS-1(121)Cs (1.1×10^{-3}). This observation suggests that small gold clusters must exist in the sublayers of the spent 0.16Au/

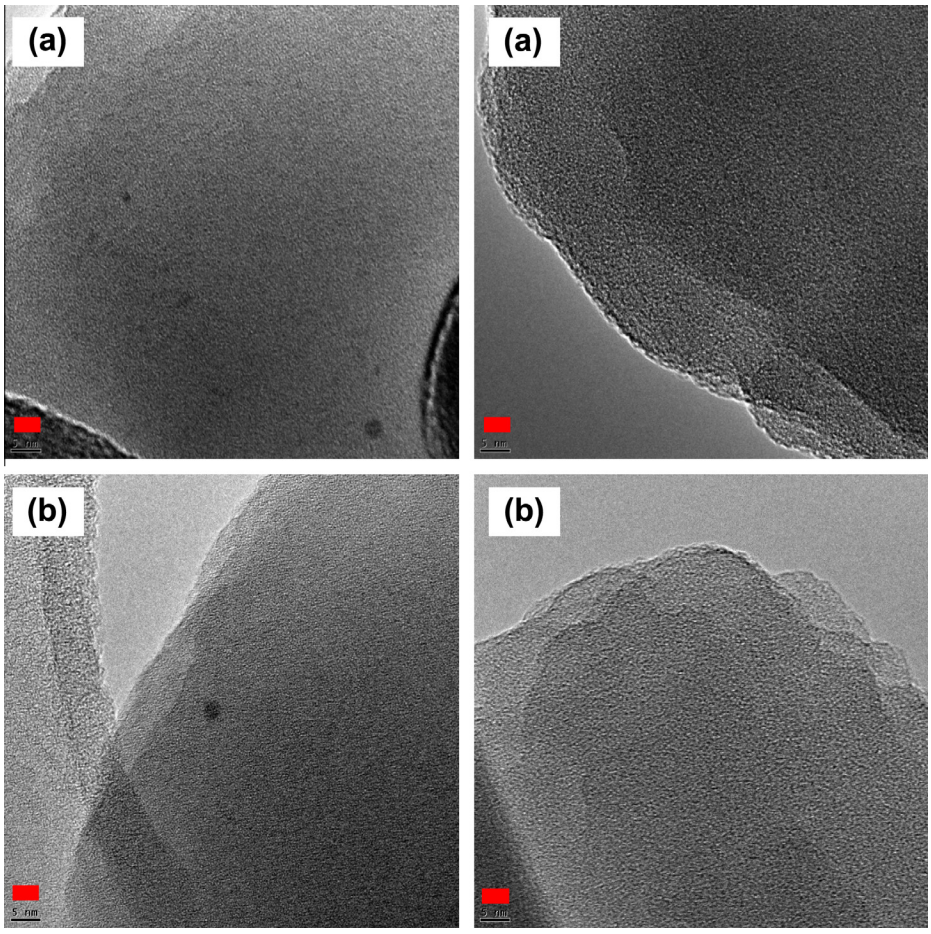

Fig. 8. TEM images of (a) fresh 0.16Au/TS-1(121)Na (b) fresh 0.16Au/TS-1(121)Cs (only few gold particles with size 2–4 nm could be found in the fresh samples). The scale bar represents 5 nm.

TS-1(121)Cs sample; since otherwise the surface Au/Si molar ratio for the spent 0.16Au/TS-1(121)Na would have been higher than that for the spent 0.16Au/TS-1(121)Cs sample.

The Au $4f_{7/2}$ line (not shown) was at ~84.4 eV for both fresh 0.16Au/TS-1(121)Cs and 0.16Au/TS-1(121)Na samples. After the reaction, however, a lower binding energy of the Au $4f_{7/2}$ photoelectron line (not shown), as compared to Au^0 at ~83.6–84 eV [45], was found in both the spent 0.16Au/TS-1(121)Cs sample (82.8 eV) and the spent 0.16Au/TS-1(121)Na sample (83.3 eV). These results are intriguing but not yet interpretable until the stability of Au species in the presence of X-rays and secondary electrons and the complicated interplay between reduced relaxation expected for small particles, the initial state effects of small particles [45,46], and electron transfer to those particles from the support or the reaction medium, and the effects of air exposure are determined in future experiments.

A cartoon, Fig 10, based on the quantitative analysis of the data illustrates how the gold species could be distributed in the 0.16Au/TS-1(121)Na and 0.16Au/TS-1(121)Cs samples before and after the reaction. Therefore, the higher rate of the Cs-promoted sample suggests that gold clusters smaller than 1 nm, which are invisible in the HRTEM analysis but could be detected via the XPS analysis, are more relevant for the PO reaction compared to the larger gold particles (>2 nm).

Although attempts to use alkali and/or alkaline earth metals as promoters to improve a PO rate per gram of catalyst have been reported [7,8,12,33,47], a significant enhancement of a PO rate has not been observed until this work. This is probably due to the need for both: (1) the correct Cs/Au molar ratio required to elucidate the strong interaction between Cs and Au and (2) the existence of the special nanoporous structure of TS-1 to induce and stabilize small gold species (<1 nm) for the PO reaction.

3.6. Effect of Ti content on PO rate

Fig. 11 shows the effect of the Ti content on the PO rate for both Au/TS-1Cs and Au/TS-1Na samples with different gold loadings. We investigated the effect of Ti content on the PO catalytic performance of Au/TS-1Na samples with different gold loadings in our previous work [9] and, surprisingly, found that the gold atom efficiency ($g_{PO}\ h^{-1}\ g_{Au}^{-1}$) of the Au/TS-1Na samples with higher Ti content was much lower than that of the Au/TS-1Na samples with lower Ti content. This is shown by the different slopes in the rate versus loading plots found for the Au/TS-1(121)Na and Au/TS-1(77)Na samples at the gold loading <0.1 wt%, shown in Fig 11 as well. However, it is interesting to note that the PO rate of the Au/TS-1(121)Cs samples was not significantly higher than that of the Au/TS-1(77)Cs samples at gold loadings <0.1 wt%, which means there was no significant difference in the gold atom efficiency for those Au/TS-1Cs samples with different Ti contents. This small difference in the gold atom efficiency for the Au/TS-1Cs samples with different Ti contents was unexpected.

3.7. Effect of Ti and Au content on PO selectivity

In our previous work, we attributed the lower rate at higher Ti content to the existence of extraframework Ti and/or very small TiOx clusters [9] since it has been reported that Ti–O–Ti entities are detrimental for the PO reaction [3,4,48]. This picture is supported by the lower PO and H_2 selectivity and higher propanal

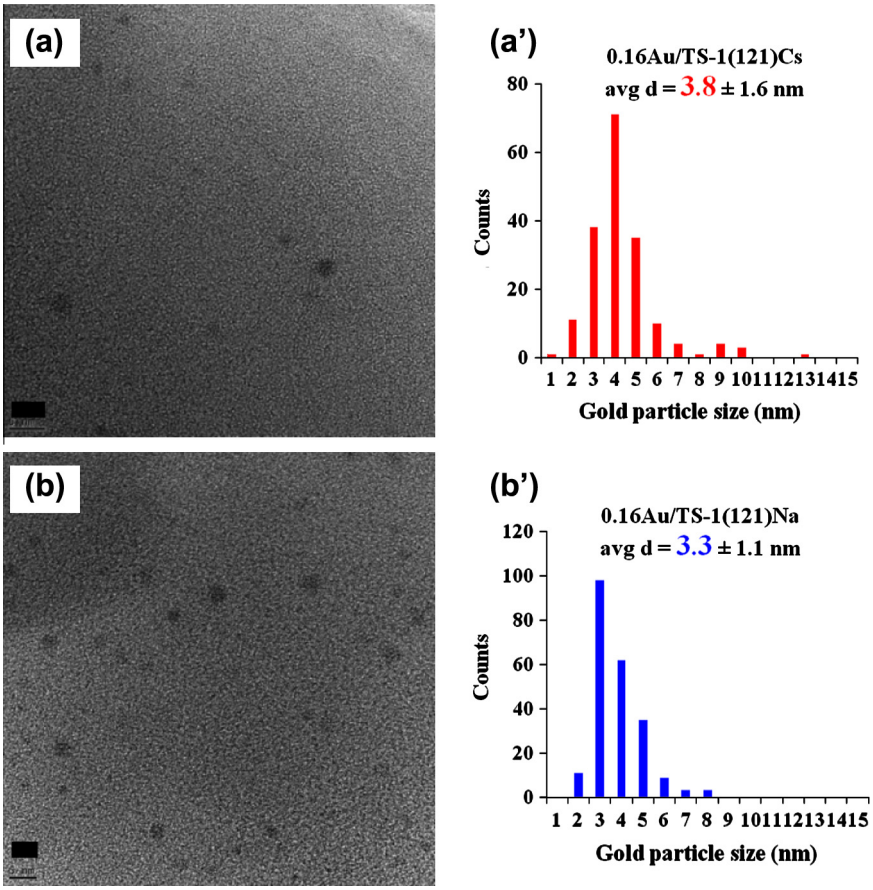

Fig. 9. TEM images of (a) spent 0.16Au/TS-1(121)Na and (b) spent 0.16Au/TS-1(121)Cs and the corresponding particle size distributions (a′ and b′). The scale bars represent 5 nm.

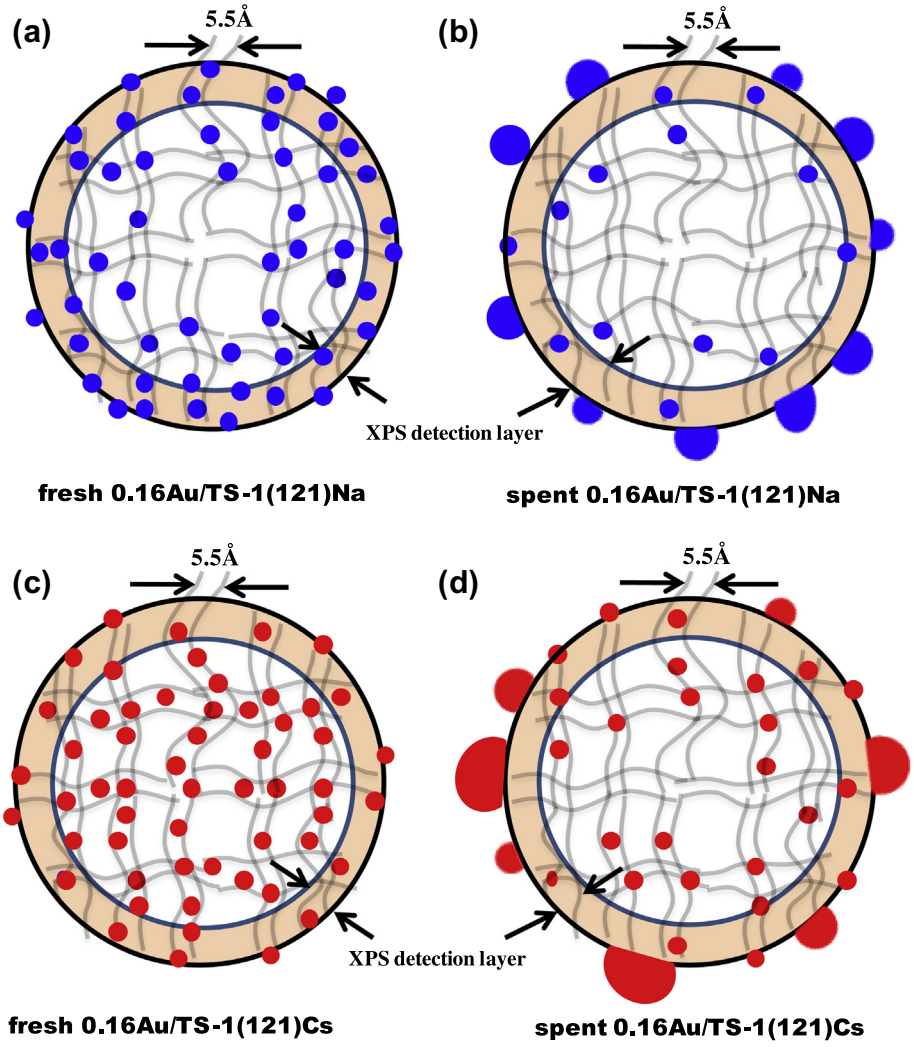

Fig. 10. Proposed model for the gold species spatial distribution (based on the XPS and TEM analysis results of the samples before and after the reaction) for (a) fresh 0.16Au/TS-1(121)Na, (b) spent 0.16Au/TS-1(121)Na, (c) fresh 0.16Au/TS-1(121)Cs, and (d) spent 0.16Au/TS-1(121)Cs. The samples were then unloaded and exposed to air prior the XPS and TEM analyses.

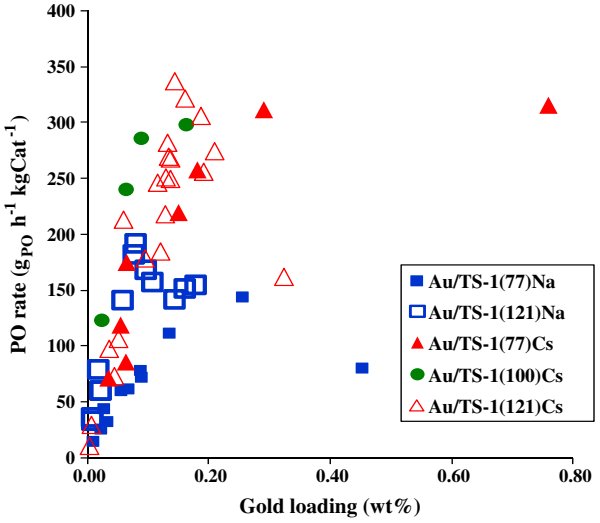

Fig. 11. PO rate per gram of catalyst for Au/TS-1 samples with different gold loadings, different Ti contents and prepared by using either Na_2CO_3 or Cs_2CO_3 as a precipitation agent. The data were taken as the average values of the first 1–2 h at ~200 °C.

(Pr) selectivity (~10%) observed in the Au/TS-1(77)Na samples, as compared to those for the Au/TS-1(121)Na samples at the gold loading <0.1 wt% (Table 3). Consistent with the rate behavior, however, neither PO nor H_2 selectivity was significantly affected by the higher Ti content for the Au/TS-1(77)Cs samples. Table 3 also shows that the PO and H_2 selectivities generally decreased as the gold loading increased (from 0.01 to 0.16 wt%) for both Au/TS-1(121)Na and Au/TS-1(121)Cs samples. The propanal (Pr) selectivity of the Au/TS-1(77)Na samples was found to be significantly higher than that of the Au/TS-1(121)Na samples regardless of the gold loading, consistent with the presence of extraframework Ti and/or small TiOx clusters [4].

For the Au/TS-1(77)Cs samples, both PO selectivities (80–87%) and propanal (Pr) selectivities (1–3%) were close to those of the Au/TS-1(121)Cs samples at the same gold loading in the range from 0.1 to 0.3 wt%, which implies that the active sites for the isomerization of PO, presumably the extraframework Ti and/or small TiOx in the TS-1, might be altered or poisoned by the presence of Cs (as we have shown there exists a interaction between Cs and Ti). The H_2 selectivity of Au/TS-1(77)Cs samples was found to be ~20–30% regardless of the gold loading and was generally higher than those of the Au/TS-1(77)Na samples (12–20%). It has been reported that

larger gold particles (~2 nm) promote the H_2 combustion [6], and we have discussed above that it is easier for the small gold clusters originally located in the nanoporous channels in the Au/TS-1(77)Na samples to move out to the external surface of the TS-1, which would facilitate the formation of larger gold particles (~2 nm) and make the H_2 selectivity of the Au/TS-1(77)Na samples lower than that of the Au/TS-1(77)Cs samples.

4. Conclusions

We have demonstrated that the Au/TS-1(121)Cs catalysts with gold loading >0.1 wt% prepared by using Cs_2CO_3 as a gold precipitation agent can have initial PO rates up to ~ 300—350 $g_{PO}\ h^{-1}\ kg_{Cat}^{-1}$ at ~200 °C, which is about *twice* the highest rate currently reported in the literature (~ 160 $g_{PO}\ h^{-1}\ kg_{Cat}^{-1}$ at ~200 °C). That PO rate decayed to ~ 260 $g_{PO}\ h^{-1}\ kg_{Cat}^{-1}$ after ~15 h at ~200 °C. This promotion is driven by a strong Cs/Au interaction which is evidenced by a four times higher gold uptake efficiency for the Au/TS-1(121)Cs versus Au/TS-1(121)Na samples, together with the XPS/TEM analyses for 0.16Au/TS-1(121)Na and 0.16Au/TS-1(121)Cs samples showing that Cs can attract and retain more gold in the TS-1 nanoporous channels, which, in turn, are shown to be necessary for promotion of the Cs/Au interaction. Based on this interaction and the premise that increasing gold loading tends to generate larger gold particles, we propose that the enhanced PO rate per gram of catalyst in high gold-loading region (>0.1 wt%) is due to the stabilization of gold clusters in the TS-1 nanoporous channels by the presence of Cs. This conclusion is also supported by the ~10% higher PO selectivity and ~5–10% higher H_2 selectivity over the Au/TS-1(121)Cs samples relative to their Na analogues in the high gold-loading region (0.1–0.16 wt%), since larger gold particles have been proposed to promote the H_2 combustion [6], CO_2 formation, and the isomerization of PO over Au/TS-1 [1]. We also showed that lower Ti content in Au/TS-1 catalysts (with either Na_2CO_3 or Cs_2CO_3 as a precipitation agent) favors PO catalytic performance. The conclusion that the number, but not the nature, of the active sites is changed by the presence of Cs is supported by the lack of change in the measured apparent activation energy for PO production. Thus, this work shows that small gold clusters inside the TS-1 nanoporous channels can be active sites for the production of PO from propylene, oxygen, and hydrogen.

5. Perspective

On the occasion of the 50th anniversary of this flagship journal, it seems appropriate to try to set this paper in the context of the evolving state-of-the-science of catalysis. This work touches on many important themes that define the current focus of the field, including new reaction pathways to industrially important products, catalysts that exploit the unique properties of nanoscale materials, spectroscopic characterization of catalyst chemistry, the quest to identify catalytic sites, and the role of theory in catalysis research. Each will be discussed in turn.

A single-step process to produce propylene oxide (PO) from propylene and oxygen with no environmentally unfriendly by-products has been a "holy grail" reaction in catalysis for decades. Haruta's discovery [16,49] that very high selectivity to PO can be achieved if hydrogen is added to the reaction mixture and catalysts containing nanosized Au particles and Ti are used opened the possibility of success. A characteristic of a true breakthrough in catalysis is the amount of subsequent research it generates. In this case, a new field has been spawned on the unique properties and reactivity of nanosized Au particles.

While direct epoxidation of ethylene by oxygen over silver catalysts has been known for years [50], these, and other catalysts that activate nucleophilic oxygen, attack the relatively weak allylic C–H bond in propylene to yield acrolein at best. Addition of hydrogen by Haruta allowed a new pathway: reaction of H_2 and O_2 to produce HOOH *in situ*, thus providing an electrophilic oxidant that can attack the double bond directly to give PO. While the logic of this chemistry was apparent early [5,16], proof of this pathway has come only slowly. Usually, one would turn to detailed chemical kinetic analysis to corroborate a mechanistic hypothesis. In this case, however, the initial catalysts were too short-lived to allow the accumulation of data at varying temperature and reactant composition that would yield activation energies, orders of reaction, and finally a sequence of elementary steps representing the reaction path. Later on, the catalyst stability was significantly improved by using a silica support with higher Ti dispersion, such as Ti-grafted silica and was attributed to the suppression of the formation of surface adsorbed species [21,48]. Spectroscopic observation of peroxy species [21,22] provided support for *in situ* hydrogen peroxide generation, and kinetic studies have recently begun to provide more detailed mechanistic support [30,31,51]. We emphasize that understanding the detailed sequence of elementary steps that describe the reaction and obtaining quantitative values for the associated rate and equilibrium constants is an essential part of understanding any catalyst/reaction system and provides a quantitative starting point for improving performance or extending the operating window. This work is not yet completed for the Au/PO system, but we note that the observation that the measured hydrogen order is roughly double that of oxygen already puts constraints on the possible sequences of elementary steps.

The biggest impact of this work has probably been through the catalyst itself. Nanosized gold particles are the quintessential example of the catalytic possibilities of the unique properties of nanoscale materials. For most reactions, including the production of PO, bulk gold (i.e., Au particles >10 nm in size, terminated primarily by low index faces) is inactive. While there is still considerable debate about the size of the most effective nano-gold catalysts, it is clear that the most interesting and potentially useful catalytic activity is associated with Au in the <2 nm size range. For CO oxidation [52,53] and the water gas-shift reaction [54,55], there is strong evidence that the coordinative unsaturation of corner and edge atoms in nanoparticles is essential for generating catalytic activity of Au. The picture is not yet as clear for the PO reaction. A long standing and interesting question in catalysis concerns the effect on catalytic activity of the electronic transition from a molecular cluster of atoms to a true metal as defined by its band structure. Recent work by Klies et al. [56] has shown that the cluster size at which this transition can be expected for Au is of the order of 560 atoms (~2.7 nm), but whether this electronic effect contributes to Au catalysis has not yet been established. It does illustrate, however, one of the reasons why the size of the most active Au particles for PO catalysis is an important question. While the work of Haruta et al. implicated that the dominant Au sites are the particles in the 2–5 nm size range for Au/TiO_2 and/or Au/Ti-based oxide catalysts [16,17] and in the 1–2 nm range for the Au/TS-1 system [15], the high activity of Au on TS-1 raised the possibility that the Au sites in the zeolite channels could be active [9,11,23], thus lowering the size to <1 nm. Proving that such is the case has only been recently achieved [24]. What seemed initially like a straightforward task was delayed by the finding that the catalytic activity in the Au/TS-1 system is accounted for a small number of very active sites [10]. While one can continue to hope that this is a relatively rare event in catalysis, its implications are profound. When the active entity is a minority species, consistent synthesis of the catalyst and ability to apply the full arsenal of spectroscopic and even microscopy characterization tools can be challenging. As the data in this paper confirm, the highest specific activity occurs in the Au/TS-1 system at the lowest Ti and Au

loadings, ruling out IR of Au-specific probe molecules for characterization, for example. The relatively large size of the TS-1 crystallites has so far prevented direct observation of Au clusters in the TS-1 pores as a way to determine their size and alteration of the state of the gold by either X-rays or secondary electrons has complicated the use of XAS or XPS as characterization tools. These restrictions on many of the standard methods for characterizing catalytic sites have limited progress in fully understanding this system. As is common in modern catalysis, however, theory can provide guidance, even when experiments are stymied. A series of DFT studies have shown that small clusters of Au can catalyze HOOH production from H_2 and O_2 [18–20,57] and that such clusters in TS-1, particularly near Ti defects [23] can produce PO by peroxide attack of propylene at a Ti site [58,59], thus supporting the hypothesis of the reaction pathway in Au/TS-1.

We see that this system has not yet yielded all its secrets to the impressive array of tools that assist modern catalysis research, but the catalytic sites are being increasingly better defined, detailed kinetic analysis has started, and theory has helped to test hypotheses about both the reaction pathway and the catalyst chemistry and structure. Interestingly, the hindrance to progress, namely the low concentration of very active sites, is also an opportunity. If a stable material with a higher density of such active sites can be synthesized, it would be an interesting catalyst indeed, both because it would be amenable to close scrutiny by a broader array of tools and for its potential for commercial production of propylene oxide.

Acknowledgments

Support from the Department of Energy, Office of Basic Energy Sciences, Chemical Sciences, under Grant DE-FG02-03ER15408 is gratefully acknowledged. The authors would also like to thank the Surface Analysis Facility at Birck Nanotechnology Center for XPS measurements and Mr. Wei-Hsuan Liu for his help and discussion of the kinetic measurements.

Appendix A. Supplementary material

Supplementary data associated with this article can be found, in the online version, at http://dx.doi.org/10.1016/j.jcat.2013.05.023.

References

[1] J.H. Huang, T. Takei, T. Akita, H. Ohashi, M. Haruta, Appl. Catal. B – Environ. 95 (2010) 430–438.
[2] T.A. Nijhuis, M. Makkee, J.A. Moulijn, B.M. Weckhuysen, Ind. Eng. Chem. Res. 45 (2006) 3447–3459.
[3] C.X. Qi, T. Akita, M. Okumura, K. Kuraoka, M. Haruta, Appl. Catal. A – Gen. 253 (2003) 75–89.
[4] E.E. Stangland, B. Taylor, R.P. Andres, W.N. Delgass, J. Phys. Chem. B 109 (2005) 2321–2330.
[5] T.A. Nijhuis, B.J. Huizinga, M. Makkee, J.A. Moulijn, Ind. Eng. Chem. Res. 38 (1999) 884–891.
[6] J.Q. Lu, X.M. Zhang, J.J. Bravo-Suarez, K.K. Bando, T. Fujitani, S.T. Oyama, J. Catal. 250 (2007) 350–359.
[7] B.S. Uphade, T. Akita, T. Nakamura, M. Haruta, J. Catal. 209 (2002) 331–340.
[8] B.S. Uphade, Y. Yamada, T. Akita, T. Nakamura, M. Haruta, Appl. Catal. A – Gen. 215 (2001) 137–148.
[9] W.-S. Lee, M.C. Akatay, E.A. Stach, F.H. Ribeiro, W.N. Delgass, J. Catal. 287 (2012) 178–189.
[10] B. Taylor, J. Lauterbach, W.N. Delgass, Appl. Catal. A – Gen. 291 (2005) 188–198.
[11] N. Yap, R.P. Andres, W.N. Delgass, J. Catal. 226 (2004) 156–170.
[12] A.K. Sinha, S. Seelan, S. Tsubota, M. Haruta, Angew. Chem.-Int. Ed. 43 (2004) 1546–1548.
[13] B. Taylor, J. Lauterbach, W.N. Delgass, Catal. Today 123 (2007) 50–58.
[14] L. Cumaranatunge, W.N. Delgass, J. Catal. 232 (2005) 38–42.
[15] J.H. Huang, E. Lima, T. Akita, A. Guzman, C.X. Qi, T. Takei, M. Haruta, J. Catal. 278 (2011) 8–15.
[16] T. Hayashi, K. Tanaka, M. Haruta, J. Catal. 178 (1998) 566–575.
[17] C.X. Qi, J.H. Huang, S.Q. Bao, H.J. Su, T. Akita, M. Haruta, J. Catal. 281 (2011) 12–20.
[18] L. Barrio, P. Liu, J.A. Rodriguez, J.M. Campos-Martin, J.L.G. Fierro, J. Phys. Chem. C 111 (2007) 19001–19008.
[19] S.M. Lang, T.M. Bernhardt, R.N. Barnett, B. Yoon, U. Landman, J. Am. Chem. Soc. 131 (2009) 8939–8951.
[20] D.G. Barton, S.G. Podkolzin, J. Phys. Chem. B 109 (2005) 2262–2274.
[21] J.J. Bravo-Suarez, K.K. Bando, J.I. Lu, M. Haruta, T. Fujitani, S.T. Oyama, J. Phys. Chem. C 112 (2008) 1115–1123.
[22] B. Chowdhury, J.J. Bravo-Suarez, N. Mimura, J.Q. Lu, K.K. Bando, S. Tsubota, M. Haruta, J. Phys. Chem. B 110 (2006) 22995–22999.
[23] A.M. Joshi, W.N. Delgass, K.T. Thomson, J. Phys. Chem. B 110 (2006) 2572–2581.
[24] W.-S. Lee, M.C. Akatay, E.A. Stach, F.H. Ribeiro, W.N. Delgass, J. Catal. 296 (2012) 31–42.
[25] R.B. Khomane, B.D. Kulkarni, A. Paraskar, S.R. Sainkar, Mater. Chem. Phys. 76 (2002) 99–103.
[26] J. Gaudet, K.K. Bando, Z.X. Song, T. Fujitani, W. Zhang, D.S. Su, S.T. Oyama, J. Catal. 280 (2011) 40–49.
[27] W.S. Lee, B.Z. Wan, C.N. Kuo, W.C. Lee, S. Cheng, Catal. Commun. 8 (2007) 1604–1608.
[28] A. Tuel, L.G. Hubert-Pfalzgraf, J. Catal. 217 (2003) 343–353.
[29] M. Du, G. Zhan, X. Yang, H. Wang, W. Lin, Y. Zhou, J. Zhu, L. Lin, J. Huang, D. Sun, L. Jia, Q. Li, J. Catal. 283 (2011) 192–201.
[30] J.Q. Lu, X.M. Zhang, J.J. Bravo-Suarez, S. Tsubota, J. Gaudet, S.T. Oyama, Catal. Today 123 (2007) 189–197.
[31] B. Taylor, J. Lauterbach, G.E. Blau, W.N. Delgass, J. Catal. 242 (2006) 142–152.
[32] B.S. Uphade, M. Okumura, S. Tsubota, M. Haruta, Appl. Catal. A – Gen. 190 (2000) 43–50.
[33] J.Q. Lu, X.M. Zhang, J.J. Bravo-Suarez, T. Fujitani, S.T. Oyama, Catal. Today 147 (2009) 186–195.
[34] X.T. Gao, S.R. Bare, J.L.G. Fierro, M.A. Banares, I.E. Wachs, J. Phys. Chem. B 102 (1998) 5653–5666.
[35] P. Ratnasamy, D. Srinivas, H. Knozinger, Adv. Catal. 48 (2004) 1–169.
[36] Y. Hasegawa, A. Ayame, Catal. Today 71 (2001) 177–187.
[37] L.B. Xiong, J.L. Li, B. Yang, Y. Yu, J. Nanomaterials 425 (2012) 117–124.
[38] A. Tuel, J. Diab, P. Gelin, M. Dufaux, J.F. Dutel, Y. Bentaarit, J. Mol. Catal. 63 (1990) 95–102.
[39] S. Maurelli, M. Vishnuvarthan, G. Berlier, M. Chiesa, Phys. Chem. Chem. Phys. 14 (2012) 987–995.
[40] L.Y. Chen, G.K. Chuah, S. Jaenicke, J. Mol. Catal. A – Chem. 132 (1998) 281–292.
[41] J. Su, G. Xiong, J.C. Zhou, W.H. Liu, D.H. Zhou, G.R. Wang, X.S. Wang, H.C. Guo, J. Catal. 288 (2012) 1–7.
[42] C.B. Khouw, M.E. Davis, J. Catal. 151 (1995) 77–86.
[43] X. Chen, W.S. Chu, D.L. Chen, Z.H. Wu, A. Marcelli, Z.Y. Wu, Chem. Geol. 268 (2009) 74–80.
[44] F. Moreau, G.C. Bond, A.O. Taylor, J. Catal. 231 (2005) 105–114.
[45] R. Radnik, C. Mohr, P. Claus, Phys. Chem. Chem. Phys. 5 (2003) 172–177.
[46] K. Chakarova, M. Mihaylov, S. Ivanova, M.A. Centeno, K. Hadjiivanov, J. Phys. Chem. C 115 (2011) 21273–21282.
[47] F.S. Wang, C.X. Qi, J.T. Ma, Catal. Commun. 8 (2007) 1947–1952.
[48] G. Mul, A. Zwijnenburg, B. van der Linden, M. Makkee, J.A. Moulijn, J. Catal. 201 (2001) 128–137.
[49] M. Haruta, B.S. Uphade, S. Tsubota, A. Miyamoto, Res. Chem. Intermed. 24 (1998) 329–336.
[50] R.A. van Santen, H. Kuipers, Adv. Catal. 35 (1987) 265–321.
[51] S.T. Oyama, X.M. Zhang, J.Q. Lu, Y.F. Gu, T. Fujitani, J. Catal. 257 (2008) 1–4.
[52] T.V.W. Janssens, B.S. Clausen, B. Hvolbaek, H. Falsig, C.H. Christensen, T. Bligaard, J.K. Norskov, Top. Catal. 44 (2007) 15–26.
[53] N. Lopez, T.V.W. Janssens, B.S. Clausen, Y. Xu, M. Mavrikakis, T. Bligaard, J.K. Norskov, J. Catal. 223 (2004) 232–235.
[54] M. Shekhar, J. Wang, W.S. Lee, W.D. Williams, S.M. Kim, E.A. Stach, J.T. Miller, W.N. Delgass, F.H. Ribeiro, J. Am. Chem. Soc. 134 (2012) 4700–4708.
[55] W.D. Williams, M. Shekhar, W.S. Lee, V. Kispersky, W.N. Delgass, F.H. Ribeiro, S.M. Kim, E.A. Stach, J.T. Miller, L.F. Allard, J. Am. Chem. Soc. 132 (2010) 14018–14020.
[56] J. Kleis, J. Greeley, N.A. Romero, V.A. Morozov, H. Falsig, A.H. Larsen, J. Lu, J.J. Mortensen, M. Dulak, K.S. Thygesen, J.K. Norskov, K.W. Jacobsen, Catal. Lett. 141 (2011) 1067–1071.
[57] D.H. Wells, W.N. Delgass, K.T. Thomson, J. Catal. 225 (2004) 69–77.
[58] A.M. Joshi, W.N. Delgass, K.T. Thomson, J. Phys. Chem. C 111 (2007) 7841–7844.
[59] D.H. Wells, W.N. Delgass, K.T. Thomson, J. Am. Chem. Soc. 126 (2004) 2956–2962.